isvr Institute of Sound and Vibration Research

Study of Regularized Solutions to Improve the Indirect Force Determination and Transfer Path Analysis Using Numerical Simulations for a Flat Plate

A.N. Thite and D.J. Thompson

ISVR Technical Memorandum 855

October 2000

University of Southampton

SCIENTIFIC PUBLICATIONS BY THE ISVR

Technical Reports are published to promote timely dissemination of research results by ISVR personnel. This medium permits more detailed presentation than is usually acceptable for scientific journals. Responsibility for both the content and any opinions expressed rests entirely with the author(s).

Technical Memoranda are produced to enable the early or preliminary release of information by ISVR personnel where such release is deemed to the appropriate. Information contained in these memoranda may be incomplete, or form part of a continuing programme; this should be borne in mind when using or quoting from these documents.

Contract Reports are produced to record the results of scientific work carried out for sponsors, under contract. The ISVR treats these reports as confidential to sponsors and does not make them available for general circulation. Individual sponsors may, however, authorize subsequent release of the material.

UNIVERSITY OF SOUTHAMPTON

INSTITUTE OF SOUND AND VIBRATION RESEARCH

DYNAMICS GROUP

Study of Regularized Solutions to Improve the Indirect Force Determination and Transfer Path Analysis Using Numerical Simulations for a Flat Plate

by

A.N. Thite and D.J. Thompson

ISVR Technical Memorandum No. 855

October 2000

Contents

1. Introduction

In transfer path analysis (TPA) [1-7] forces are usually identified indirectly from an accelerance matrix and a set of operational accelerations. The measurements of accelerances (measured from source locations to the response locations) and operational responses (measured at a series of locations due to the operational source), however, involve errors which are magnified by the matrix inversion particularly at frequencies where the condition number of the accelerance matrix is high. This ultimately leads to errors in estimates of the contributions from these forces via different paths to the response. Hence it is important that the forces are identified reliably for the TPA to produce reliable results.

The force identification errors can generally be reduced by over-determination, i.e using a larger number of responses than the forces to be identified, and employing a least square error solution. The least square error solution can be accomplished by Moore-Penrose pseudo-inversion [5]. In such a least square solution, however, it is observed that the errors in force reconstruction continue to be large at frequencies where the accelerance matrix is ill-conditioned. This can, for example, be due to the fact that only a small number of modes contribute significantly to the operational responses close to resonances; this number can be smaller than the number of forces to be identified [8] (over-determination, by adding extra response points does not help under this situation).

The least square solution can also be acheived through singular value decomposition of the accelerance matrix. It is possible in this case to discard insignificant singular values in order to improve the effective condition number of the accelerance matrix and hence improve the force identification. The singular values can be discarded based on the error

in the estimation of accelerances [1,5] or the error in the measurement of operational accelerations [6,7]. As seen in [5,6], however, singular value rejection does not overcome the large force reconstruction error in the vicinity of antiresonance and the individual contribution from each force may contain large errors when a smaller number of modes (less than number of forces) are contributing to the responses even though the overall response might be accurate.

For a long time in the field of digital image processing and more recently in relation to Nearfield Acoustic Holography (NAH), other techniques have been employed to improve source reconstruction [9-12]. These include iterative techniques of inversion and Tikhonov regularization. In these techniques instead of minimising a cost function based on ordinary least square errors, a function which incorporates some bias is introduced. This new function is minimised to identify the source. In both techniques, the error in the force reconstruction is divided into the bias error and the magnified variance. In the ordinary least square solution only the variance is magnified and no bias error is introduced. There can be a large magnification of the variance at frequencies where the accelerance matrix is ill-conditioned. By introducing a bias error which increases with the value of a eg regularization parameter, it is observed that there exists a point (value of regularization parameter or number of iterations) where the bias error and the random error cross over. For larger values the bias error dominates, for smaller values the random error dominates. At the cross over point the cost function is minimised. The introduction of a bias error limits the magnification of random errors in the accelerance and the operational responses. This however comes at the cost of a small bias error in the force reconstruction.

In this report these two techniques are used in a numerical simulation of a TPA application in which the test object is a rectangular simply supported flat plate [5,6]. Four simulatneous coherent forces are considered and five responses are used to reconstruct them.

The Tikhonov regularization is used to reconstruct the forces in chapter 2 where the theory for this also discussed. The iterative technique and its implemation are explained in chapter 3.

2. Tikhonov regularization

2.1 Introduction

The ordinary least square solution for the inverse problem (force reconstruction) generally results in large force reconstruction errors at frequencies where the accelerance matrix has a high condition number. Under such circumstances, it is possible to improve the reconstruction by 'regularizing' the solution. One type of regularization which has already been studied [5-6] is singular value rejection based on the error norm. Other regularization methods are based on the introduction of bias in the solution. This is explained below, which follows [10-12].

The observed operational responses (accelerations) $\hat{a}$ can be represented as

$$\hat{a} = a + e$$

where a is the response and e is the measurement error vector, or

$$\hat{a} = AF + e$$

where A - Matrix of theoretical accelerances

F - A force vector

However, an additional error $\tilde{e}$ can be identified, that is due to the matrix inversion. The reconstructed forces $\hat{F}$ can be used with the measured FRF matrix, $\hat{A}$ to calculate the operational responses:

$$\tilde{a} = \hat{A}\hat{F} + \tilde{e}$$

The least square solution (eg the Moore-Penrose pseudo-inverse) aims to determine $\hat{F}$ such that the fitting errors $\tilde{e}$ are minimised i.e.

$$\min(\tilde{e}^H\tilde{e}) \qquad \text{or} \qquad \min\sum_{i=1}^{m}\tilde{e}_i^2$$

These fitting errors may come from error in $\hat{A}$, errors in $\hat{a}$ or errors in the model used (eg additional inputs)

2.2 Tikhonov regularization

Instead of ordinary least square solution, Tikhonov suggested [16,10-12] minimising a cost function given by

$$J = \min[(\tilde{e}^H\tilde{e}) + \lambda(\hat{F}^H\hat{F})] \tag{1}$$

where λ is a regularization parameter. This cost function introduces a bias into the solution which can be adjusted (by varying λ value) to limit the magnification of measurement errors due to ill-conditioning. Therefore, expanding J

$$J = (\hat{a} - \hat{A}\hat{F})^H(\hat{a} - \hat{A}\hat{F}) + \lambda(\hat{F}^H\hat{F})$$

$$= \hat{a}^H\hat{a} - \hat{a}^H\hat{A}\hat{F} - \hat{F}^H\hat{A}^H\hat{a} + \hat{F}^H\hat{A}^H\hat{A}\hat{F} + \hat{F}^H\lambda\hat{F}$$

$$= \hat{F}^H(\hat{A}^H\hat{A} + I\lambda)\hat{F} - \hat{a}^H\hat{A}\hat{F} - \hat{F}^H\hat{F}^H\hat{a} + \hat{a}^H\hat{a}$$

$$= \hat{F}^H(\hat{A}^H\hat{A} + I\lambda)\hat{F} - \hat{a}^H\hat{A}\hat{F} - \hat{F}^H(\hat{a}^H\hat{A})^H + \hat{a}^H\hat{a}$$

or

$$J = \hat{F}^H B\hat{F} - b^H\hat{F} - \hat{F}^H b + c \tag{2}$$

where

$$B = (\hat{A}^H\hat{A} + I\lambda), \qquad b = \hat{A}^H\hat{a} \qquad \text{and} \qquad c = \hat{a}^H\hat{a}$$

The optimal solution which reduces the force reconstruction errors can be derived by minimising the cost function (2). For this cost function to be minimum, the first derivative of 'J' with respect to force vector $\hat{F}$ must be zero. As the terms in the cost function contain complex variables it is necessary that it be separated into real and imaginary parts [13]. Therefore using

$$B = B_R + iB_I$$

$$\hat{F} = F_R + iF_I$$

$$b = b_R + ib_I$$

the first term in (2) can be expanded as, (noting that **B** is a Hermitian matrix)

$$\hat{F}^H B \hat{F} = (F_R + iF_I)^H (B_R + iB_I)(F_R + iF_I)$$

$$= ({F_R}^T - i{F_I}^T)(B_R + iB_I)(F_R + iF_I)$$

$$= ({F_R}^T B_R + i{F_R}^T B_I - i{F_I}^T B_R + {F_I}^T B_I)(F_R + iF_I)$$

$$= {F_R}^T B_R F_R + i{F_R}^T B_I F_R - i{F_I}^T B_R F_R + {F_I}^T B_I F_R + i{F_R}^T B_R F_I - {F_R}^T B_I F_I + {F_I}^T B_R F_I + i{F_I}^T B_I F_I$$

(3)

The above equation can be simplified as follows :

I. Since the imaginary part of **B** is skew symmetric

${F_R}^T B_I F_R = 0$ and ${F_I}^T B_I F_I = 0$ This eliminates the 2nd and 8th terms

II. Since $({F_R}^T B_R F_I)^T = {F_I}^T B_R F_R$ and ${F_I}^T B_R F_R$ is a real scalar , ${F_R}^T B_R F_I = {F_I}^T B_R F_R$

This eliminates the 3rd and 5th terms

and

III. Since $({F_R}^T B_I F_I)^T = -{F_I}^T B_I F_R$ and ${F_I}^T B_I F_R$ is a real scalar, ${F_R}^T B_I F_I = -{F_I}^T B_I F_R$

So the 4th and 6th terms are equal

Therefore (3) can be written as

$$J = F_R{}^T B_R F_R + F_I{}^T B_R F_I - 2F_R{}^T B_I F_I - b^H \hat{F} - \hat{F}^H b + c$$

The fourth and fifth terms in this equation can be expanded to give,

$$-b^H \hat{F} - \hat{F}^H b = -(b_R^T F_R + ib_R^T F_I - ib_I^T F_R + b_I^T F_I + F_R^T b_R + iF_R^T b_I - iF_I^T b_R + F_I^T b_I)$$

Since all the terms represent scalar real numbers

$$-b^H \hat{F} - \hat{F}^H b = -(2b_R^T F_R + 2b_I^T F_I)$$

Therefore the simplified version of cost function is written as

$$J = F_R{}^T B_R F_R + F_I{}^T B_R F_I - 2F_R{}^T B_I F_I - (2b_R^T F_R + 2b_I^T F_I) + c \qquad (4)$$

Now the cost function can be differentiated with respect to each of the real and imaginary components.

$$\frac{\partial J}{\partial F_R} = \left(\frac{\partial J}{\partial F_{1R}}, \frac{\partial J}{\partial F_{2R}}, \ldots\ldots \frac{\partial J}{\partial F_{nR}} \right)^T$$

$$\frac{\partial J}{\partial F_I} = \left(\frac{\partial J}{\partial F_{1I}}, \frac{\partial J}{\partial F_{2I}}, \ldots\ldots \frac{\partial J}{\partial F_{nI}} \right)^T$$

Following the derivation in [13], use can be made of various properties of such derivatives, two of which are given below

$$\frac{\partial(\phi^T \alpha)}{\partial \alpha} = \phi \quad \text{and} \quad \frac{\partial(\alpha^T X \alpha)}{\partial \alpha} = (X + X^T)\alpha \quad \text{where } \phi \text{ and } X \text{ are independent of } \alpha.$$

In the second relation if 'X' is symmetric then

$$\frac{\partial(\alpha^T X \alpha)}{\partial \alpha} = 2X\alpha$$

Using the above two properties, the derivatives can be written as

$$\frac{\partial J}{\partial F_R} = 2B_R F_R - 2B_I F_I - 2b_R \qquad (5)$$

$$\frac{\partial J}{\partial F_I} = 2B_R F_I + 2B_I F_R - 2b_I \qquad (6)$$

Using the concept of a complex gradient 'g' ,

$$g = \frac{\partial J}{\partial F_R} + i\frac{\partial J}{\partial F_I}$$

$$g = 2B_R F_R - 2B_I F_I - 2b_R + i2B_R F_I + i2B_I F_R - i2b_I$$

For a minimum value of 'J', g has to be equal to zero. Therefore

$$2(B_R F_R + iB_R F_I + iB_I F_R - B_I F_I) - 2(b_R + ib_I) = 0$$

The first term in the above equation is simply BF, therefore

$$2(B\hat{F} - b) = 0$$

and hence the optimal solution which minimises the error amplification in force reconstruction is given by

$$\hat{F} = B^{-1} b$$

By expanding **B** the solution can also be written as

$$\hat{F} = (\hat{A}^H \hat{A} + I\lambda)^{-1} \hat{A}^H \hat{a} \qquad (7)$$

To obtain insight into this solution and in order to compare it with pseudo-inversion, (7) can be represented in terms of the singular values of the accelerance matrix, where $\hat{A} = USV^H$

$$\hat{F} = ((USV^H)^H USV^H + I\lambda)^{-1}(USV^H)^H \hat{a}$$

$$= (VS^H SV^H + VI\lambda V^H)^{-1} VS^H U^H \hat{a} \qquad \text{since } U^H U \text{ and } VV^H \text{ are unitary matrices}$$

$$= (V(S^H S + I\lambda)V^H)^{-1} VS^H U^H \hat{a}$$

$$\hat{F} = V(S^H S + I\lambda)^{-1} S^H U^H \hat{a} \qquad (8)$$

This can be compared with the pseudo-inversion in which $\hat{F} = VS^{-1}U^H \hat{a}$. In (8) the term $(S^H S + I\lambda)^{-1} S^H$ is a diagonal matrix having elements $\frac{S_{ii}}{(s_{ii}^2 + \lambda)}$, which replaces the S^{-1} the terms of which are s_{ii}^{-1}.

As can be seen from the above relation, the regularization parameter effectively modifies the singular values in the inverse. In doing this it introduces a bias error into the solution. When the condition number of the accelerance matrix is high, the effect of smaller singular values which are prone to errors can be nullified by choosing an appropriate regularization value λ. If it is a constant value for each of the frequencies, when associated with high condition number, the effect of adding the optimal regularization parameter to larger singular values results in minimal bias. However, it is essential to choose a proper regularization value so that it results in minimum magnification of measurement errors while introducing negligible bias in the solution. To do this, it is necessary to know the errors in the measurement or use mathematical methods which approximate the optimal regularization parameter. One of the mathematical concepts to choose regularization parameters when errors in the measurement are not known is explained below.

2.3 Ordinary cross validation

This method was suggested by Allen [14]. In this method, out of 'm' responses only 'm-1' are used in the force identification. The forces so identified are then used in reconstructing the remaining response. This can be done for different values of regularization parameter. The closeness of reconstruction of this response indicates the

effectiveness of the chosen regularization parameter. This method is also referred to as the PRESS method ('Prediction sum of squares' of deviations). The procedure followed is given below

1. The number of responses 'm' measured is ensured to be at least one more than the number of forces. Start with zero value of λ, and identify the forces based on the m-1 set of responses using (7). Let the number of forces reconstructed be 'p'. Using these forces reconstruct the remaining response.

Writing $\hat{F}_k$ - Identified force with kth element of response left out, etc,

the square of the deviation is $\left(\hat{a}_k - \hat{A}_k \hat{F}_k\right)^2$

where

$\hat{A}_k$ - is a FRF row vector containing the transfer paths from 'p' force locations to the kth response location.

2. This procedure of leaving out one response and calculating the sum of squares of deviations is repeated for each one of the response elements in turn. Based on the above deviations, the 'PRESS' is calculated for that value of λ (initially λ=0)as

$$PRESS(\lambda) = \frac{1}{m}\sum_{k=1}^{m}\left(\hat{a}_k - \hat{A}_k \hat{F}_k\right)^2 \qquad (9)$$

3. The above steps are repeated for different values of λ (gradually increasing the value). The value of λ which gives smallest 'PRESS' is the optimum value of regularization parameter for that frequency.

There are other techniques that can be used to select the regularization parameter [17], such as

a. Generalised cross validation

b.Deterministic constrained least squares

c. Equivalent degrees of freedom

However these are not investigated further here.

2.4 Force reconstruction

The following strategies are compared for force reconstruction in this chapter

1. Use of full rank matrix (all singular values used)

2. Singular value rejection based on the norm of accelerance error matrix (as in [5]). Based on the analysis in [5] the rejection threshold is set to +/- one standard deviation of the accelerance error.

3. Resampling of accelerances (full rank matrix) as in [5] i.e. a new set of accelerances is taken for each sample of operational response.

4. Tikhonov regularized solution based on ordinary cross validation

In all the simulations four sources and five responses are used. The test structure is a flat plate 0.6 x 0.5 x 0.0015 m , as used in [5,6]. The accelerances estimated using 50 averages where as operational accelerations are obtained using 25 averages.

The forces are reconstructed by the inversion of the accelerance matrix and using operational accelerations as in [5-6]. Figures 1a-d show the reconstructed force 1 for all the four cases. As expected the force reconstruction errors are large when all singular values are used (Figure 1a). The improvement is considerable when singular values are rejected based on the norm of error matrix (compare Figures 1a and 1b). Figure 1c shows the force 1 reconstructed with resampling of the accelerance matrix [5]. In the high frequency range it is comparable to the singular value rejection case. It results in large errors near the first resonance, but the results are better than when all singular values are

used without resampling. The reconstruction of force 1 obtained using Tikhonov regularization is shown in Figure 1d. The reconstruction is overestimated at the first resonance but is closer to the actual force in most of the frequency range.

Figures 2a-d show the reconstructed force 2. The overestimates in force 2 are larger than for force 1 (Figure 2a) when all singular values are used (as force 2 is smaller than force 1). For the low frequency region the improvement is considerable when singular values are rejected based on the norm of the accelerance error matrix (Figure 2b). At most of the frequencies, however, force 2 is still overestimated, with a peaky reconstruction near the first resonance. Figure 2c shows the reconstruction of force 2 from resampling of the accelerance matrix. The degree of overestimation in the reconstruction is more than that when singular values are rejected but far better than when all singular values are used. The Tikhonov regularization based reconstruction of force 2 is similar to the singular value rejection case (Figure 2d).

Figures 3a-d show the reconstructed force 3. The singular value rejection based reconstruction along with Tikhonov regularized solution result have the smallest errors (Figures 3b,d). The resampling case results in greater errors than the above but less than when all singular values are used without resampling.

Figures 4a-d show the reconstructed force 4. The reconstruction errors for force 4 are large compared to all the other forces (Figure 4a) when all singular values are used (force 4 is the smallest of all). Even the other strategies also result in higher errors. The reconstruction error is relatively low when singular values are rejected or the solution is Tikhonov regularized (Figures 4b and 4d).

Overall, the reconstruction errors are minimum with Tikhonov regularization based on ordinary cross validation in the higher frequency range and the second best is singular value rejection case.

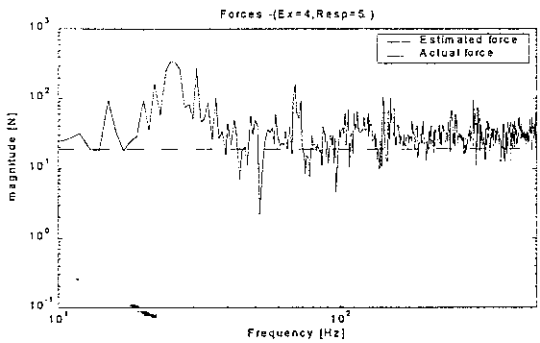

Figure 1a. Force 1 for all singular values used for 4 sources and 5 responses

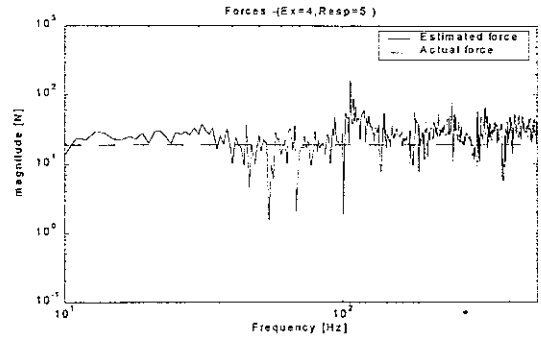

Figure 1b. Force 1 with singular value rejection based on +/- one standard deviation for 4 sources and 5 responses

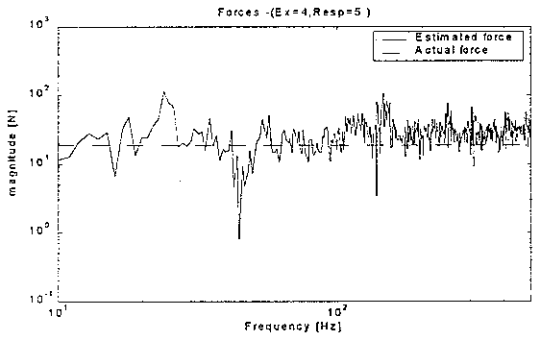

Figure 1c. Force 1 for all singular values used with resampling for 4 sources and 5 responses

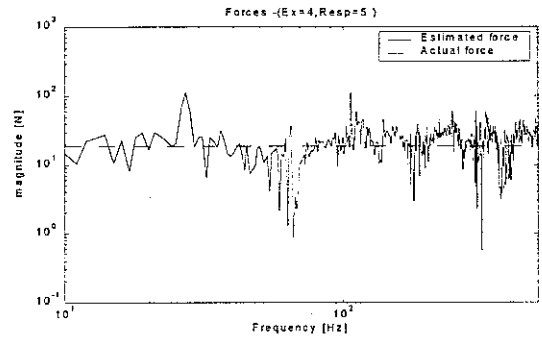

Figure 1d. Force 1 with Tikhonov regularization for 4 sources and 5 responses

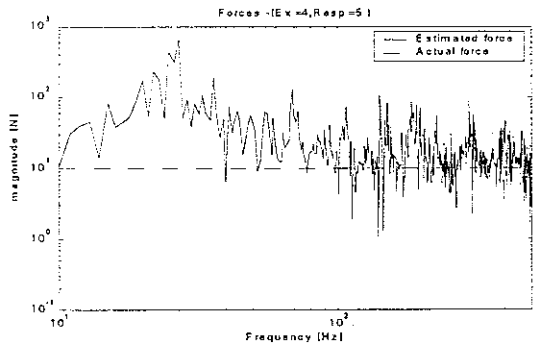

Figure 2a. Force 2 for all singular values used for 4 sources and 5 responses

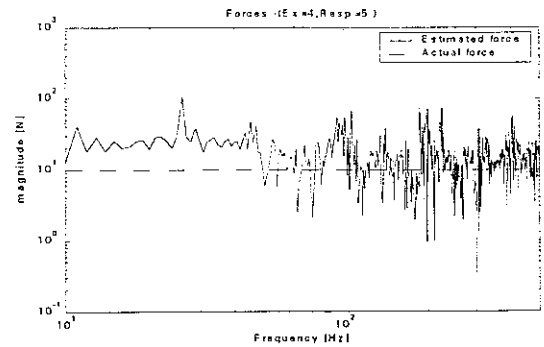

Figure 2b. Force 2 with singular value rejection based on +/- one standard deviation for 4 sources and 5 responses

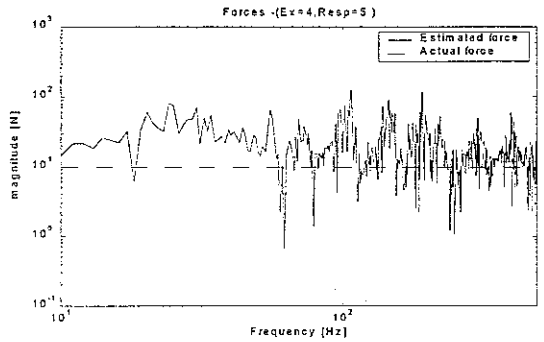

Figure 2c. Force 2 for all singular values used with resampling for 4 sources and 5 responses

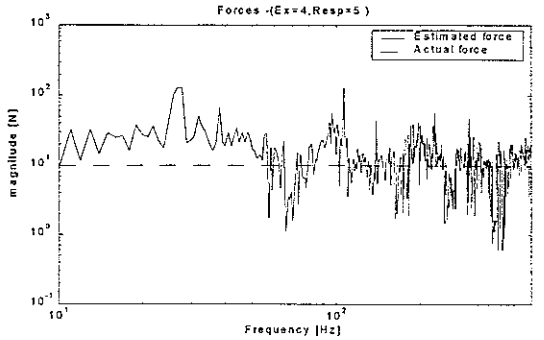

Figure 2d. Force 2 with Tikhonov regularization for 4 sources and 5 responses

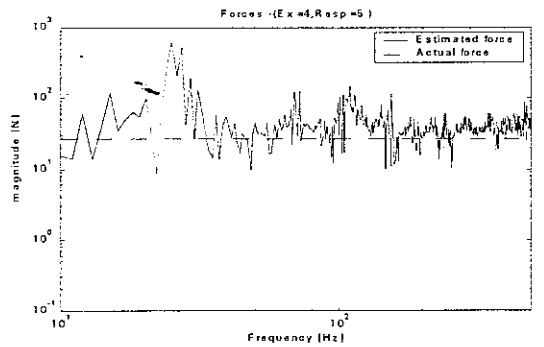

Figure 3a. Force 3 for all singular values used for 4 sources and 5 responses

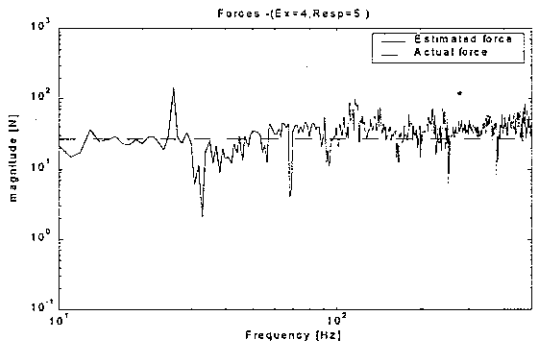

Figure 3b. Force 3 with singular value rejection based on +/- one standard deviation for 4 sources and 5 responses

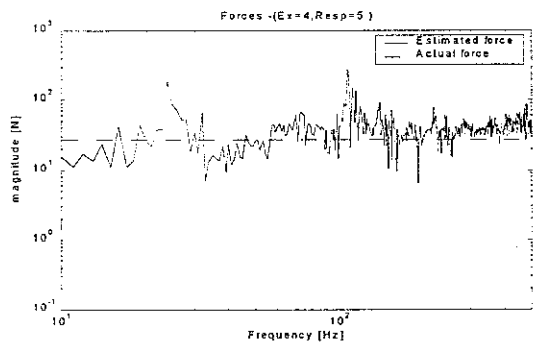

Figure 3c. Force 3 for all singular values used with resampling for 4 sources and 5 responses

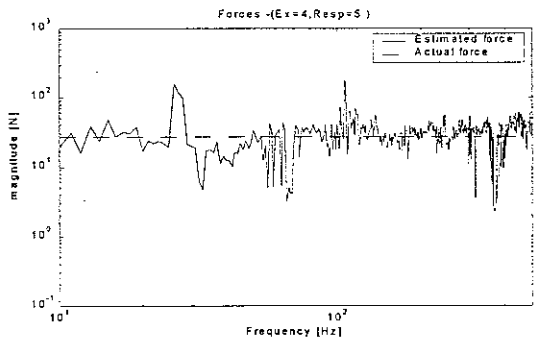

Figure 3d. Force 3 with Tikhonov regularization for 4 sources and 5 responses

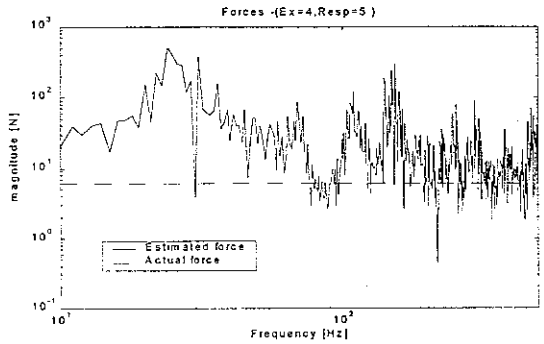

Figure 4a. Force 4 for all singular values used for 4 sources and 5 responses

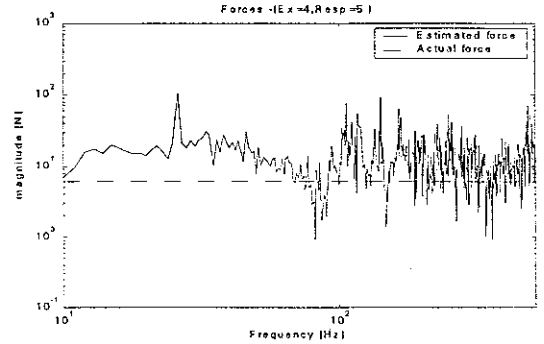

Figure 4b. Force 4 with singular value rejection based on +/- one standard deviation for 4 sources and 5 responses

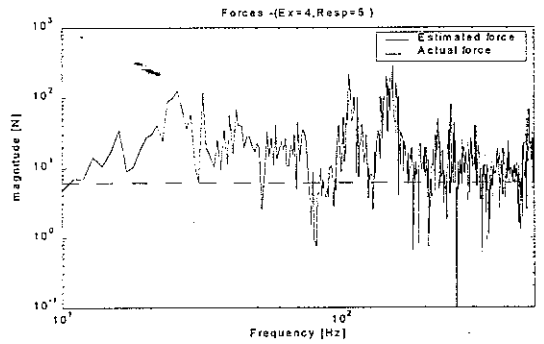

Figure 4c. Force 4 for all singular values used with resampling for 4 sources and 5 responses

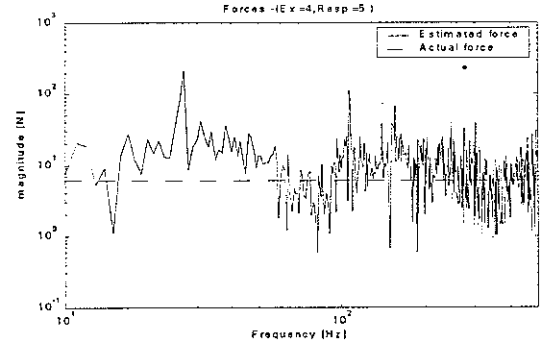

Figure 4d. Force 4 with Tikhonov regularization for 4 sources and 5 responses

The force reconstruction is also shown in 1/3 octave representation in Figures 5a-d. Again the superiority of the Tikhonov regularization and the singular value rejection case is confirmed in the results.

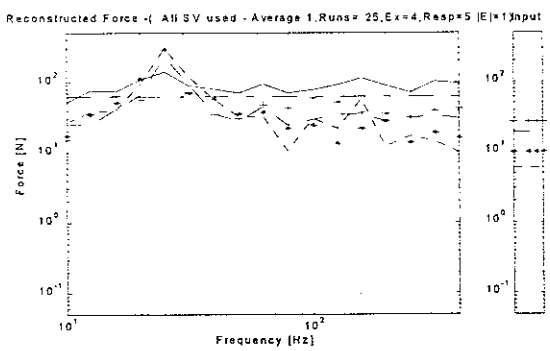

Figure 5a. 1/3 octave band reconstructed forces - all singular values used for 4 sources and 5 responses

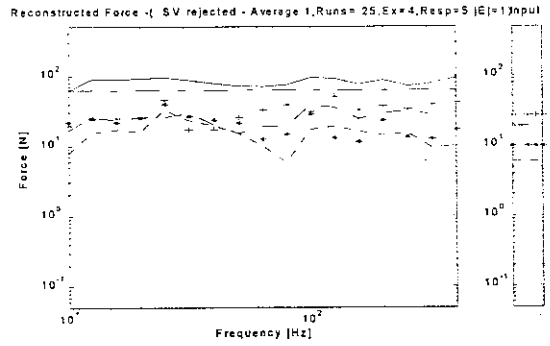

Figure 5b. 1/3 octave band reconstructed forces with singular value rejection based on +/- one standard deviation for 4 sources and 5 responses

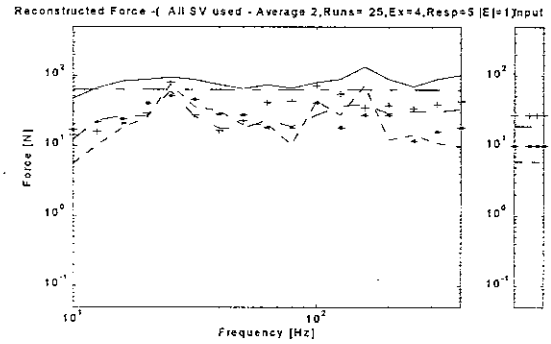

Figure 5c. 1/3 octave band reconstructed forces - all singular values used with resampling for 4 sources and 5 responses

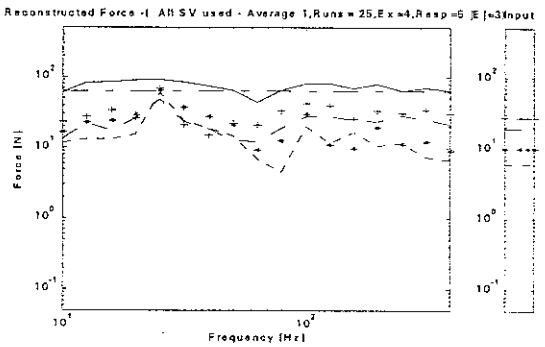

Figure 5d. 1/3 octave band reconstructed forces - Tikhonov regularization for 4 sources and 5 responses

2.5 Velocity at the receiver location

Figures 6a-d show the 1/3 octave band velocity response contribution at the receiver location from force 1. The velocity contribution calculated with Tikhonov regularization results in the smallest error compared to all other strategies (compare 6d with 6a-c). When all singular values are used the velocity contribution is overestimated to a large extent (Figure 6a). When resampling is combined with the use of all singular values the result improves (compare Figures 6c and 6d).

Figures 7a-d show the 1/3 octave band velocity response contribution at the receiver location from force 2. As the force 2 reconstruction is very poor (overestimated) in all the cases, the velocity contribution is larger than the actual result. However, Tikhonov regularization again results in the smallest errors (compare Figure7d and Figures7a-c).

Figures 8a-d show the 1/3 octave band velocity response contribution at the receiver location from force 3. Once more the velocity contribution calculated with Tikhonov regularization has smaller errors than all other strategies (compare 6d with 6a-c). When singular values are rejected, the prediction is close to that predicted by Tikhonov regularization (Figure 8b).

Figures 9a-d show the 1/3 octave band velocity response contribution at the receiver location from force 4. As the force 4 has the smallest amplitude and largest relative reconstruction error (overestimated) in all cases, the velocity contribution is larger than the actual one. It is very poor when all singular values are used without resampling (Figure 9a). However, Tikhonov regularization results in a better prediction than the others (compare Figure 9d and Figures 9a-c).

The total velocity response due to all four forces is shown in Figures 10a-d. In all the cases between the resonances the prediction is poor. In fact it is higher than the actual response in these frequency ranges. As expected (due to better individual force contribution estimates), Tikhonov regularization results in the smallest errors (compare Figures 10d and Figures 10a-c). This is more evident when the velocity responses are represented in 1/3 octave bands as shown in Figure 11.

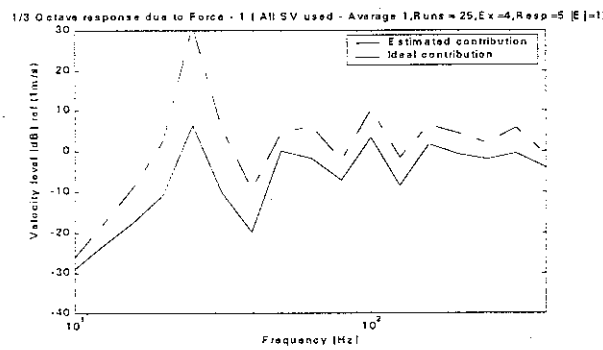

Figure 6a. 1/3 octave velocity response contribution from Force -1 for all singular values used

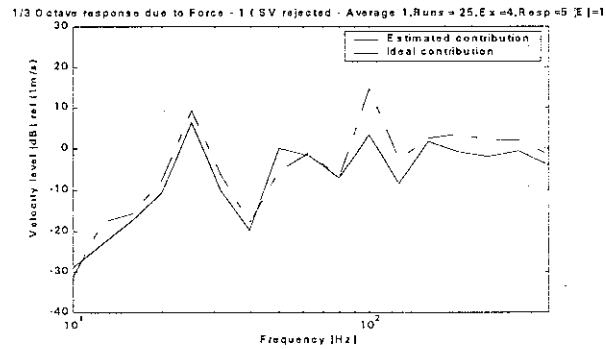

Figure 6b. 1/3 octave velocity response contribution from Force -1 for singular value rejection based on +/- one standard deviation

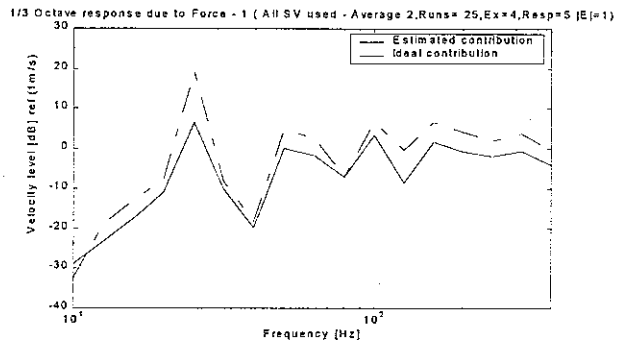

Figure 6c. 1/3 octave velocity response contribution from Force -1 for all singular values used with resampling

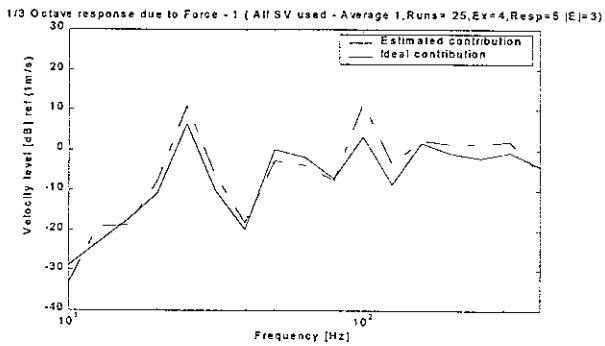

Figure 6d. 1/3 octave velocity response contribution from Force -1 for Tikhonov regularization

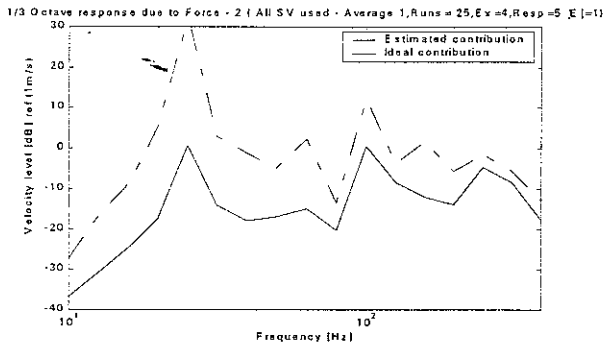

Figure 7a. 1/3 octave velocity response contribution from Force -2 for all singular values used

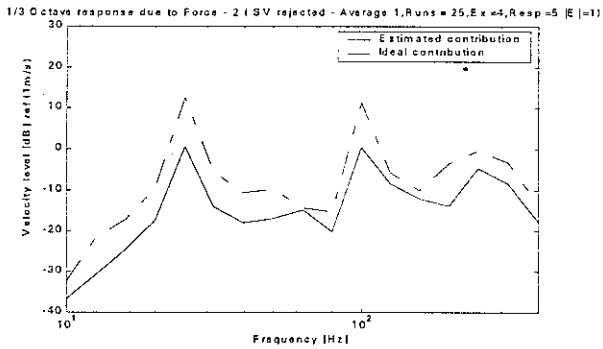

Figure 7b. 1/3 octave velocity response contribution from Force -2 for singular value rejection based on +/- one standard deviation

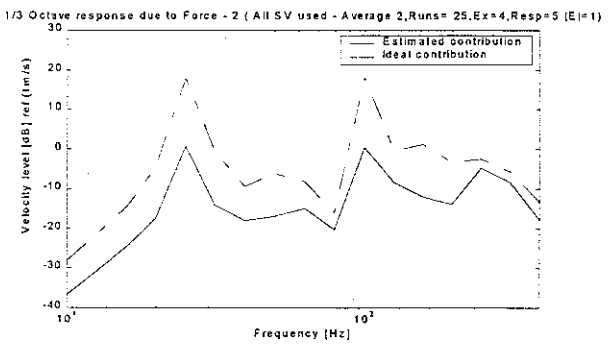

Figure 7c. 1/3 octave velocity response contribution from Force -2 for all singular values used with resampling

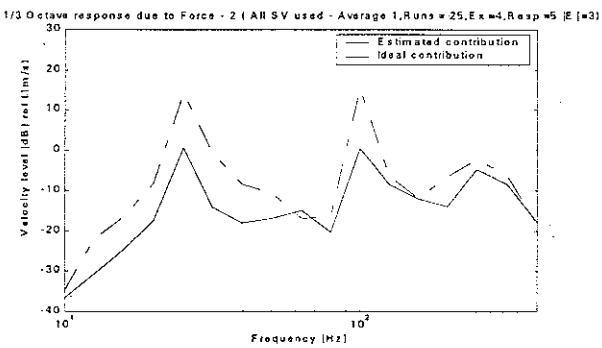

Figure 7d. 1/3 octave velocity response contribution from Force -2 for Tikhonov regularization

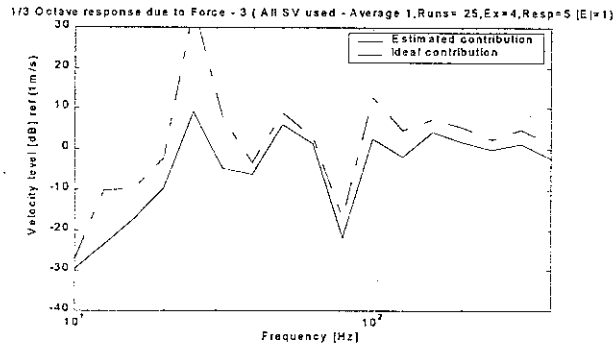

Figure 8a. 1/3 octave velocity response contribution from Force -3 for all singular values used

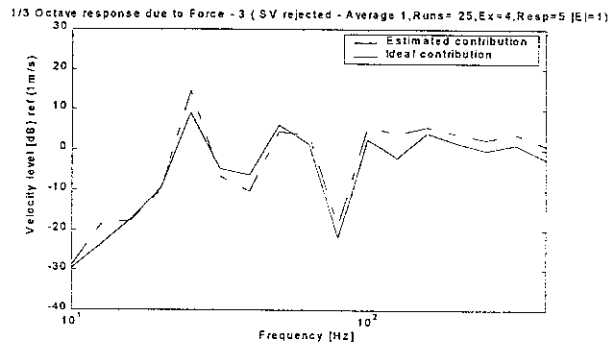

Figure 8b. 1/3 octave velocity response contribution from Force -3 for singular value rejection based on +/- one standard deviation

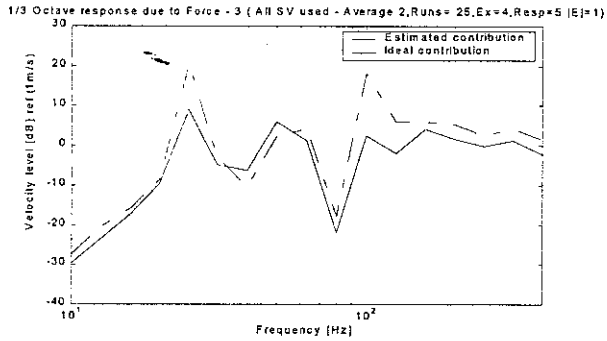

Figure 8c. 1/3 octave velocity response contribution from Force -3 for all singular values used with resampling

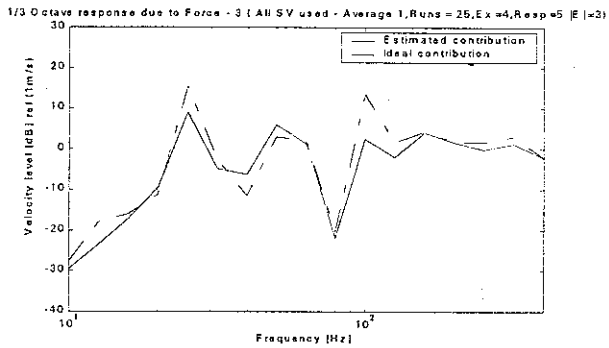

Figure 8d. 1/3 octave velocity response contribution from Force -3 for Tikhonov regularization

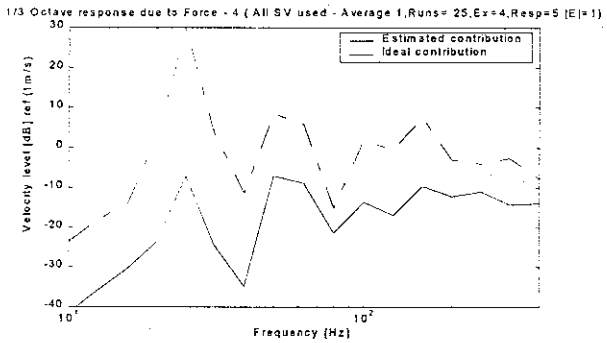

Figure 9a. 1/3 octave velocity response contribution from Force -4 for all singular values used

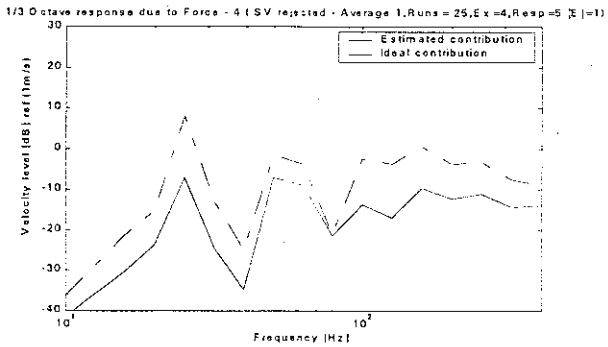

Figure 9b. 1/3 octave velocity response contribution from Force -4 for singular value rejection based on +/- one standard deviation

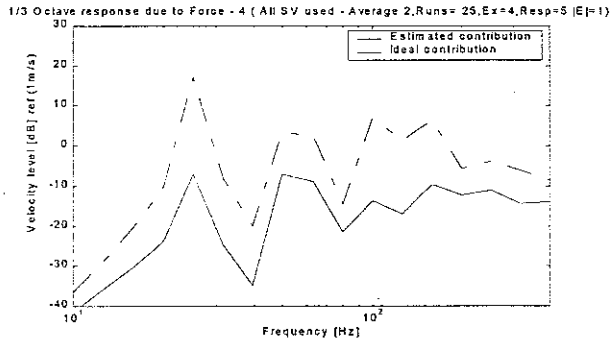

Figure 9c. 1/3 octave velocity response contribution from Force -4 for all singular values used with resampling

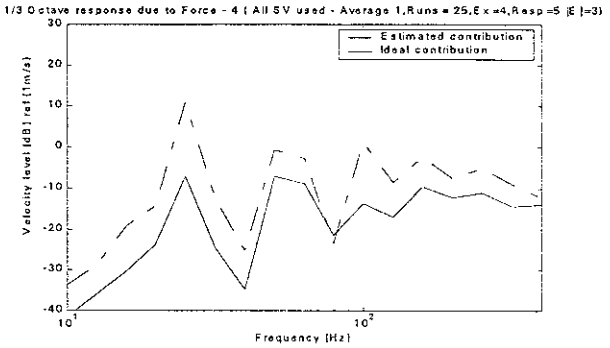

Figure 9d. 1/3 octave velocity response contribution from Force -4 for Tikhonov regularization

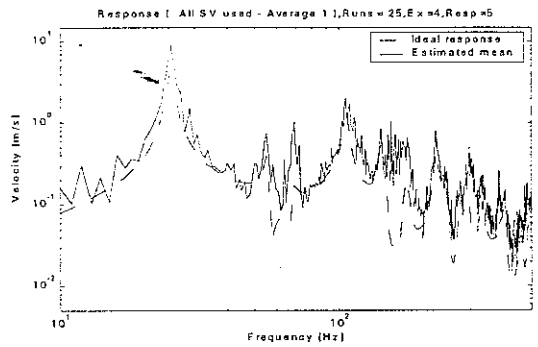

Figure 10a. Velocity response at the receiver location for all singular values used

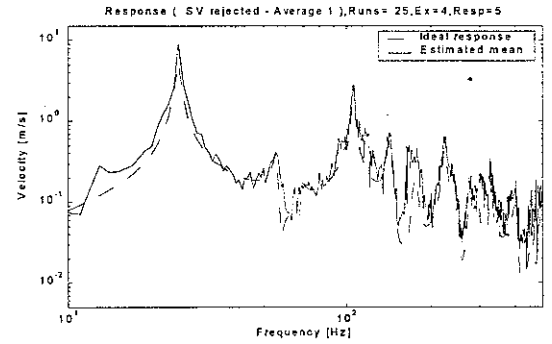

Figure 10b. Velocity response at the receiver location for singular values rejection based on +/- one std. deviation

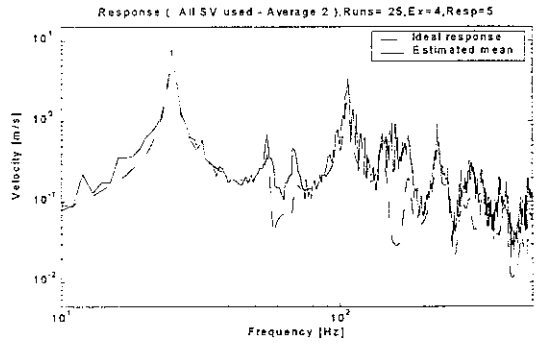

Figure 10c. Velocity response for all singular values used with resampling

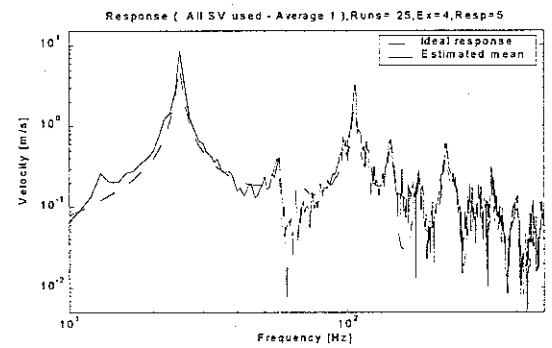

Figure 10d. Velocity response at the receiver location for Tikhonov regularization

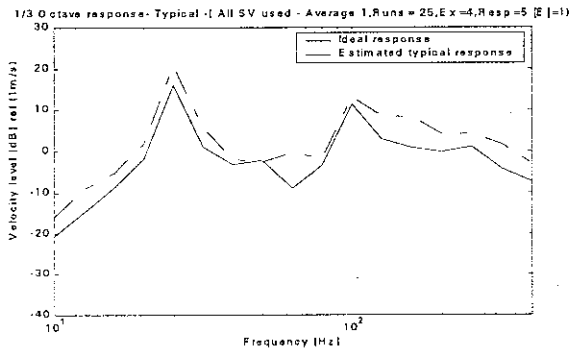

Figure 11a. 1/3 octave band velocity response for all singular values used

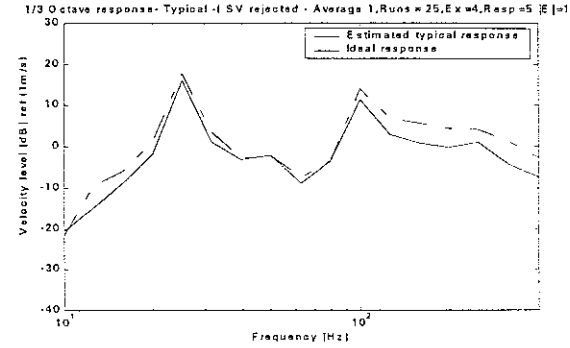

Figure 11b. 1/3 octave velocity response at the receiver location for singular values rejection based on +/- one std. deviation

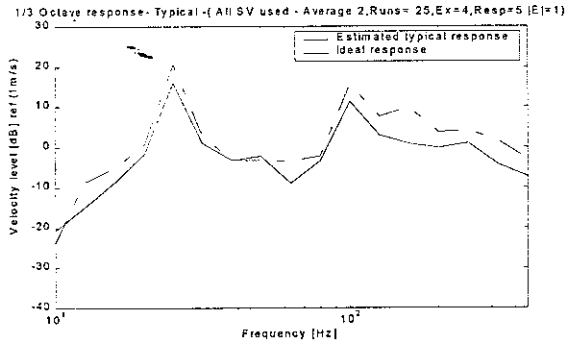

Figure 11c. 1/3 octave band velocity response for all singular values used with resampling (without phase information)

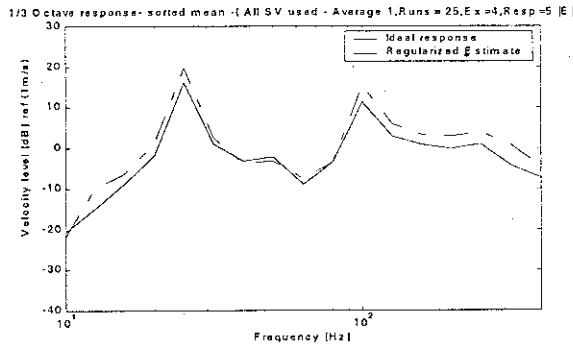

Figure 11d. 1/3 octave band velocity response for Tikhonov regularization

3.6 Summary

Using an example of a 5 x 4 FRF matrix it has been shown that Tikhonov regularization with ordinary cross validation gives superior results to singular value rejction or matrix resampling.

To quantify the above comparison, the table 1 given below shows the average 1/3 octave band error (in dB) in the velocity prediction by each of the methods.

Table 1 - Summary of results (Average 1/3 octave band errors in dB)

Method	Force 1 (19N) contribution	Force 2 (10N) contribution	Force 3 (27N) contribution	Force 4 (6N) contribution	Total contribution	Rank
Moore-Penrose	8.9	14.29	7.2	17.5	4.9	4
Resampling	4.9	8.9	2.9	14.4	4.4	3
SV rejection	3.5	6.4	2.7	8.2	3.4	2
Tikhonov Regularzn	3.0	6.3	2.8	8.0	2.5	1

3. Iterative inversion

3.1 Background

When an ill-conditioned accelerance matrix is directly inverted, the measurement errors in the operational responses are magnified in the identified forces. To overcome this, the solution could be regularized as discussed in the last chapter. In this chapter an alternative known as iterative inversion is studied. The solution in this case is based on the principle that when an infinite number of iterations is used in a proper formulation, the solution tends to the exact one. In the iteration process errors in the force identification can be classified into two groups; bias error and variance around the mean. The bias error in the forces tends to zero as the number of iterations is increased, while the random error goes on increasing. By seeking a compromise in the bias error it is possible to limit the variance. In fact, there is an optimum number of iterations where the bias error and the random error are equal. At this iteration number, the combined error reaches a minimum. This property of iterative inversion can be effectively utilized to reduce the combined error.

3.2 Derivation

Iterative inversion [9] can be applied to force identification as follows.

Given a k^{th} estimate of the forces, $\hat{F}_k$, the $k+1^{th}$ estimate is generated as

$$\hat{F}_{k+1} = \hat{F}_k + \beta \hat{A}^H \left(\hat{a} - \hat{A} \hat{F}_k \right)$$

where the term in brackets is the difference between the reconstructed response $\hat{A}\hat{F}$ and the measured response $\hat{a}$ which is multiplied by the convergence factor β.

$$\hat{F}_{k+1} = \beta \hat{A}^H \hat{a} + \left(I - \beta \hat{A}^H \hat{A} \right) \hat{F}_k \qquad (10)$$

The first approximation for the force vector is taken as

$$\hat{F}_o = \beta \hat{A}^H \hat{a}$$

Therefore from (10)

$$\hat{F}_1 = \beta \hat{A}^H \hat{a} + \left(I - \beta \hat{A}^H \hat{A} \right) \beta \hat{A}^H \hat{a}$$

and

$$\hat{F}_2 = \beta \hat{A}^H \hat{a} + \left(I - \beta \hat{A}^H \hat{A} \right) \beta \hat{A}^H \hat{a} + \left(I - \beta \hat{A}^H \hat{A} \right) \left(I - \beta \hat{A}^H \hat{A} \right) \beta \hat{A}^H \hat{a} \qquad (11)$$

and so on.

Equation (11) is a geometric series with a geometric ratio of $\left(I - \beta \hat{A}^H \hat{A} \right)$.

Therefore since $1 + n + n^2 +, \ldots\ldots + n^k = \dfrac{\left(1 - n^{k+1}\right)}{(1-n)}$,

the k^{th} term can be written as

$$\hat{F}_k = \beta \left(I - \left(I - \beta \hat{A}^H \hat{A} \right) \right)^{-1} \left(I - \left(I - \beta \hat{A}^H \hat{A} \right)^{k+1} \right) \hat{A}^H \hat{a} \qquad (12)$$

The solution converges for an infinite number of iterations only when

$$\left(I - \beta \hat{A}^H \hat{A} \right)^{k+1} \rightarrow [0] \quad \text{as} \quad k \rightarrow \infty$$

In the limitting case (when k tends to infinity), therefore from (12)

$$\hat{F}_\infty = \beta \left(\beta \hat{A}^H \hat{A} \right)^{-1} \hat{A}^H \hat{a}$$

$$= \left(\hat{A}^H \hat{A} \right)^{-1} \hat{A}^H \hat{a}$$

This is the Moore-Penrose pseudo inverse which minimizes the mean square error

$$\left| \hat{A} \hat{F}_\infty - \hat{a} \right|^2$$

3.3 Alternative formulation

For simplicity (11) can also be written as

$$\hat{F}_k = \beta \sum_{r=0}^{k} \left(I - \beta \hat{A}^H \hat{A} \right)^r \hat{A}^H \hat{a} \tag{13}$$

Using singular value decomposition of the matrix $\hat{A}$

$$\hat{F}_k = \beta \sum_{r=0}^{k} \left(I - \beta V \Lambda^2 V^H \right)^r \hat{A}^H \hat{a}$$

where $\hat{A} = USV^H$

$$\Lambda^2 = S^T S$$

$$\hat{F}_k = \beta \sum_{r=0}^{k} \left(VV^H - \beta V \Lambda^2 V^H \right)^r \hat{A}^H \hat{a} \tag{14}$$

Note $\left(VV^H - \beta V \Lambda^2 V^H \right)^r = V\left(I - \beta \Lambda^2 \right) V^H . V\left(I - \beta \Lambda^2 \right) V^H ..... V\left(I - \beta \Lambda^2 \right) V^H$

$$= V\left(I - \beta \Lambda^2 \right)^r V^H \quad \text{since } V^H V = I$$

Therefore (14) can be written as

$$\hat{F}_k = \beta \sum_{r=0}^{k} V\left(I - \beta \Lambda^2 \right)^r V^H \hat{A}^H \hat{a}$$

Again using SVD

$$= \beta \sum_{r=0}^{k} V\left(I - \beta \Lambda^2 \right)^r V^H VSU^H \hat{a},$$

$$= \beta \sum_{r=0}^{k} V\left(I - \beta\Lambda^2\right)^r SU^H \hat{a}$$

This equation can be simplified using geometric series as

$$\hat{F}_k = \beta V\left(I - \left(I - \beta\Lambda^2\right)^{k+1}\right)\left(I - \left(I - \beta\Lambda^2\right)\right)^{-1} SU^H \hat{a}$$

$$= V\left(I - \left(I - \beta\Lambda^2\right)^{k+1}\right)S^{-1}U^H \hat{a}$$

As the term in brackets, and S, are diagonal matrices this can be written as

$$\hat{F}_k = V diag\left(\frac{\left(1-\left(1-\beta s_1^2\right)^{k+1}\right)}{s_1}, \ldots\ldots\ldots\ldots \frac{\left(1-\left(1-\beta s_n^2\right)^{k+1}\right)}{s_n}\right)U^H \hat{a} \qquad (15)$$

where n is the rank of accelerance matrix.

Equation (15) can be further simplified as

$$\hat{F}_k = V diag\left(\psi_1, \psi_2, \ldots\ldots\ldots\ldots \psi_n\right)U^H \hat{a} \qquad (16a)$$

where

$$\psi_i = \frac{\left(1-\left(1-\beta s_i^2\right)^{k+1}\right)}{s_i} \qquad \text{for i=1,2,.....n} \qquad (16b)$$

Thus iterative inversion can be seen as an alternative means of regularizing the inverse of $\hat{A}$, replacing s_i^{-1} by $\psi_i(k)$.

3.4 Basis for number of iterations

To find out the optimum number of iterations in order minimize the combined error it is necessary to formulate an expression for the bias error and the variance. The expressions can be derived as follows [15].

The reconstructed operational accelerations derived from identified forces are given by

$$\tilde{a} = \hat{A}\hat{F}_k = USV^H V diag(\psi_1, \psi_2, \ldots\ldots\ldots\ldots \psi_n) U^H \hat{a}$$

$$= U diag(\phi_1, \phi_2, \ldots\ldots\ldots\ldots \phi_n) U^H \hat{a} \quad \text{where } \phi_i = \left(1 - \left(1 - \beta s_i^2\right)^{k+1}\right) \tag{17b}$$

$$= \delta_k \hat{a} \qquad \text{where } \delta_k = U diag(\phi_1, \phi_2, \ldots\ldots\ldots\ldots \phi_n) U^H \tag{17b}$$

Therefore the overall mean square error of the estimation is given by

MSE$= \varepsilon_k^{\,2} = E\left[(\tilde{a} - a)^H (\tilde{a} - a)\right]$ where $a = AF$ is the exact operational response

$$= E\left[(\delta_k \hat{a} - AF)^H (\delta_k \hat{a} - AF)\right]$$

$$= E\left[\left|\delta_k \hat{a}\right|^2\right] + |AF|^2 - E\left[\left(\delta_k \hat{a}\right)^H\right] AF - (AF)^H E\left[\delta_k \hat{a}\right]$$

$$= E\left[\left|\delta_k \hat{a}\right|^2\right] + |AF|^2 - 2\,\mathrm{Re}\left\{E\left[\left(\delta_k \hat{a}\right)^H\right] AF\right\}$$

Adding and subtracting $\left|E\left[\delta_k \hat{a}\right]\right|^2$ to this equation gives

$$\varepsilon_k^{\,2} = E\left[\left|\delta_k \hat{a}\right|^2\right] - \left|E\left[\delta_k \hat{a}\right]\right|^2 + \left|E\left[\delta_k \hat{a}\right]\right|^2 + |AF|^2 - 2\,\mathrm{Re}\left\{E\left[\left(\delta_k \hat{a}\right)^H\right] AF\right\}$$

Since (assuming the measurement of $\hat{a}$ is unbiased) $\left(E\left[\delta_k \hat{a}\right]\right) = \delta_k AF$, the first two terms in the equation can be simplified as

$$E\left[\left|\delta_k \hat{a}\right|^2\right] - \left|E\left[\delta_k \hat{a}\right]\right|^2 = E\left[\left|\delta_k \hat{a}\right|^2\right] + |\delta_k AF|^2 - 2\,\mathrm{Re}\left\{\left(E\left[\delta_k \hat{a}\right]\right)^H \delta_k AF\right\}$$

$$= E\left[\left(\delta_k \hat{a} - \delta_k AF\right)^H \left(\delta_k \hat{a} - \delta_k AF\right)\right]$$

Similarly the last three terms can be simplified as

$$\left|E\left[\delta_k \hat{a}\right]\right|^2 + |AF|^2 - 2\,\mathrm{Re}\left\{E\left[\left(\delta_k \hat{a}\right)^H\right]AF\right\} = |\delta_k AF|^2 + |AF|^2 - 2\,\mathrm{Re}\left\{\left(\delta_k AF\right)^H AF\right\}$$

$$= \left(\delta_k AF - AF\right)^H \left(\delta_k AF - AF\right)$$

Therefore the expression for MSE can be written as

$$\varepsilon_k{}^2 = E\left[\left(\delta_k \hat{a} - \delta_k AF\right)^H \left(\delta_k \hat{a} - \delta_k AF\right)\right] + \left(\delta_k AF - AF\right)^H \left(\delta_k AF - AF\right)$$

$$= E\left[\left(\delta_k \left\{\hat{a} - AF\right\}\right)^H \left(\delta_k \left\{\hat{a} - AF\right\}\right)\right] + \left(\left(\delta_k - I\right)AF\right)^H \left(\left(\delta_k - I\right)AF\right)$$

$$= E\left[trace\left\{\left(\delta_k \left\{\hat{a} - AF\right\}\right)\left(\delta_k \left\{\hat{a} - AF\right\}\right)^H\right\}\right] + \left(AF\right)^H \left(\delta_k - I\right)^H \left(\delta_k - I\right)AF$$

$$= E\left[trace\left\{\delta_k \left(\hat{a} - AF\right)\left(\hat{a} - AF\right)^H \delta_k{}^H\right\}\right] + \left(AF\right)^H \left(\delta_k - I\right)^H \left(\delta_k - I\right)AF \quad (18)$$

If it can be assumed that same variance σ^2 exists for all the measurement points, this reduces to

$$\varepsilon_k^2 = \sigma^2 \sum_{i=1}^{n} \phi_i^2 + \left(AF\right)^H \left(\delta_k - I\right)^H \left(\delta_k - I\right)\left(AF\right) \quad (19)$$

where ϕ is defined in (17a).

The above equation cannot be quantified since 'F' is unknown. The second term, however, can be simplified as follows.

The actual bias error is given by $b = \left(\delta_k - I\right)\left(AF\right)$

whilst, the estimated bias error is given by $\hat{b} = \left(\delta_k - I\right)\left(\hat{a}\right)$

The variance of the estimated bias error from the true bias error can be obtained (assuming $E\left[\hat{b}\right]=b$) as

$$E\left[\left(\hat{b}-b\right)^{H}\left(\hat{b}-b\right)\right]=E\left[\left(\hat{a}-AF\right)^{H}\left(\delta_k-I\right)^{H}\left(\delta_k-I\right)\left(\hat{a}-AF\right)\right] \tag{20}$$

$$=E\left[trace\left(\left(\left(\delta_k-I\right)\left(\hat{a}-AF\right)\right)\left(\left(\delta_k-I\right)\left(\hat{a}-AF\right)\right)^{H}\right)\right]$$

$$=E\left[trace\left(\left(\delta_k-I\right)\left(\hat{a}-AF\right)\left(\hat{a}-AF\right)^{H}\left(\delta_k-I\right)^{H}\right)\right]$$

Again with the assumption that the variance σ^2 is the same for all the acceleration measurements, the above equation can be simplified as

$$E\left[\left(\hat{b}-b\right)^{H}\left(\hat{b}-b\right)\right]=E\left[\sigma^2 trace\left(U\left(diag\left(\phi_1,..\phi_n\right)-I\right)\left(diag\left(\phi_1,..\phi_n\right)-I\right)^{H}U^{H}\right)\right]$$

$$=E\left[\sigma^2 trace\left(U\left\{diag\left(\phi_1^2,..\phi_n^2\right)-2diag\left(\phi_1,..\phi_n\right)+I\right\}U^{H}\right)\right]$$

$$=\sigma^2\left(\sum_{i=1}^{n}\phi_i^2-2\sum_{i=1}^{n}\phi_i+n\right) \tag{21}$$

The left hand side of (21) can also be simplified as

$$E\left[\left(\hat{b}-b\right)^{H}\left(\hat{b}-b\right)\right]=E\left[\hat{b}^{H}\hat{b}\right]+E\left[b^{H}b\right]-2\,\mathrm{Re}\left\{E\left[\hat{b}^{H}b\right]\right\}$$

As it has already been assumed that $E\left[\hat{b}\right]=b$, therefore

$$E\left[\left(\hat{b}-b\right)^{H}\left(\hat{b}-b\right)\right]=E\left[\hat{b}^{H}\hat{b}\right]-b^{H}b$$

Using (21)

$$E\left[\hat{b}^H \hat{b}\right] - b^H b = \sigma^2\left(\sum_{i=1}^{n}\phi_i^2 - 2\sum_{i=1}^{n}\phi_i + n\right)$$

$$\Rightarrow \qquad b^H b = E\left[\hat{b}^H \hat{b}\right] - \left\{\sigma^2\left(\sum_{i=1}^{n}\phi_i^2 - 2\sum_{i=1}^{n}\phi_i + n\right)\right\} \tag{22}$$

Combining the above equation with the earlier expression (19)

$$\varepsilon_k^2 = \sigma^2\left(2\sum_{i=1}^{n}\phi_i - n\right) + E\left[\hat{b}^H \hat{b}\right]$$

Since

$$E\left[\hat{b}^H \hat{b}\right] = \hat{b}^H \hat{b} \tag{23}$$

the mean square error can finally be written as

$$\varepsilon_k^2 = \sigma^2\left(2\sum_{i=1}^{n}\phi_i - n\right) + \hat{b}^H \hat{b} \tag{24}$$

The above expression is used in arriving at a compromise between the bias error and the variance. This can be readily established by expanding the terms in (24) as below

$$\varepsilon_k^2 = \sigma^2\left(2\sum_{i=1}^{n}\phi_i\right) - n\sigma^2 + \left(\hat{a}\right)^H U\left(diag(\phi_1,\ldots\phi_n) - I\right)^H \left(diag(\phi_1,\ldots\phi_n) - I\right)U^H\left(\hat{a}\right)$$

The second term in this equation is a constant value which does not change with the number of iterations 'k'. The cross over occurs when the first term equals the third term and where the magnification of random errors starts dominating i.e

$$\sigma^2\left(2\sum_{i=1}^{n}\phi_i\right) = \left(\hat{a}\right)^H U\left(diag(\phi_1,\ldots\phi_n) - I\right)^H \left(diag(\phi_1,\ldots\phi_n) - I\right)U^H\left(\hat{a}\right)$$

The iteration number 'k' which results in the above condition is the optimum iteration number which gives a compromise between bias error and the magnified random errors.

This iteration number can be used in (16) to obtain the reconstructed forces with minimum error.

3.5 Convergence parameter - β

The convergence parameter β decides how fast the solution is going to converge to the Moore-Penrose pseudo inversion. The larger the value of convergence parameter, the faster is the convergence. As already mentioned, however for convergence to occur the following condition has to be satisfied

$$\left(I - \beta \hat{A}^{H} \hat{A}\right)^{k+1} \rightarrow [0] \quad \text{as} \quad k \rightarrow \infty$$

The above expression decides the upper limit for the convergence parameter. Using singular value decomposition, this convergence criterion can also be written as

$\left(1 - \beta s_i^2\right) < 1$ for i=1,2,.....n.

Therefore $\beta < \frac{1}{s_i^2}$

If only one convergence parameter value β is used for all singular values, the part of the solution contributed by the larger singular values converges faster than the smaller ones. The difference increases as the condition number increases. Since in the case of high condition number, smaller singular values are prone to modification by measurement errors, the slower convergence can be effectively utilised in restricting the iteration to reduce the error propagation. To accommodate the above criterion, the convergence parameter can be written as

$\beta = \frac{c}{s_1^2}$ where c is a constant less than one.

To improve the resolution i.e enough number of iterations, it is necessary that the convergence parameter constant 'c' has different values for different condition numbers. This is because at smaller condition numbers if a large constant is used the cut-off iteration occurs at a very low iteration number. This is found to reduce the resolution. Hence the constant 'c' can be varied based on the condition number. The following exponential expression has been devised for use in the simulations in this study

$$c = 1 - 0.99e^{-\gamma\kappa}$$

where

κ - Condition number of the accelerance matrix

γ - Constant which controls exponential decay, in this study it is taken to be 0.1

The above expression is also represented graphically as shown in Figure 12.

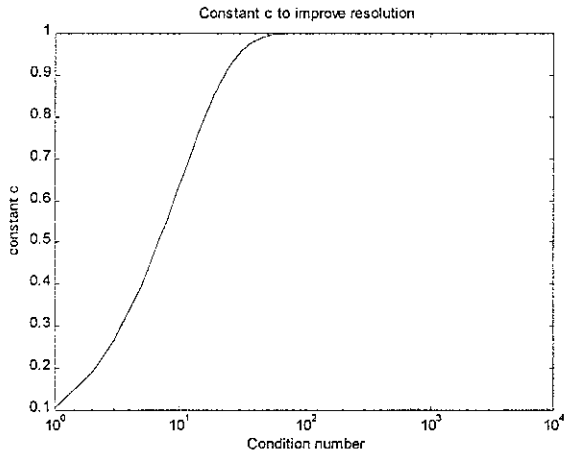

Figure 12. Variation of 'c' for $\gamma = 0.1$

3.6 Noise in the operational responses

The standard deviation in the operational response can be obtained either directly (by averaging) or indirectly as in [14]. Based on this standard deviation, the cut-off iteration number can be determined. There is a difficulty in choosing the cut-off iteration number by error compromise when the standard deviation is larger than or considerable in

magnitude compared to the response itself (eg at antiresonance). In this situation, based on the error expression it is observed that the cut-off criterion is satisfied already at the first iteration. This results in an underestimation of the forces concerned. Another problem is faced at resonance where the standard deviation is very small compared to the operational response which might lead to a larger number of iterations being required for error equalization (bias and variance). A large number of iterations means larger amplification of measurement errors. Hence the force reconstruction would be incorrect in both cases.

This problem can be overcome if a fixed percentage of the operational response is taken as the assumed standard deviation (10% or 20% etc of response), which introduces a small bias in the response predicted at the receiver location. This strategy results in another problem however, that of finding the fraction of operational response to be used as the assumed standard deviation. In this study a solution is proposed in which the reconstructed forces are used to validate operational responses other than the ones used for force reconstruction. For this, the fraction is varied in some range (10 to 50%) in small steps (5% step) and the fraction which results in small validation error at each frequency is used for force reconstruction at those frequencies. The expression for the validation error is given below

$$VE = \sum_{j=1}^{m} \frac{\left| \left| \left(\tilde{a} \right)_{valid} \right|_j - \left| \left(\hat{a} \right)_{valid} \right|_j \right|}{\left| \left(\hat{a} \right)_{valid} \right|_j}$$

where m is number of validating responses used

$\left(\tilde{a} \right)_{valid}$ - Vector of reconstructed validating operational responses

$\left(\hat{a}\right)_{valid}$ - Vector of measured validating operational responses

In the derivation of the total error in reconstruction, it is assumed that the standard deviation in the measurement of operational responses is same for all the responses. To generalize further, it is possible to incorporate individual standard deviation in the measurement of operational responses with minor modification in the formulation given in equations (19), (20), (22) and (23) as below

$$\varepsilon_k^2 = E\left[trace\left\{ \delta_k \left(\hat{a} - AF\right)\left(\hat{a} - AF\right)^H \delta_k{}^H \right\} \right]$$

$$+E\left[trace\left(\left(\delta_k - I\right)\left(\hat{a} - AF\right)\left(\hat{a} - AF\right)^H \left(\delta_k - I\right)^H \right) \right] - \hat{b}^H \hat{b}$$

The above equation can be simplified using a covariance matrix 'a' as

$$\varepsilon_k^2 = trace\left(\delta_k COV(a) \delta_k{}^H\right) + trace\left\{ \left(\delta_k - I\right) COV(a) \left(\delta_k - I\right)^H \right\} - \hat{b}^H \hat{b} \qquad (25)$$

The following strategies are compared for force reconstruction in this chapter

1. Common standard deviation for all the responses estimated from measurements.

2. Individual standard deviations for each of the responses estimated from measurments (equation (25) - values on the diagonal of COV(a) are used).

3. 25% of response as the standard deviation.

4. Standard deviation chosen in the range of 10 to 50% of response along with validation.

In all the simulations the same flat plate is used as previously with four sources and five responses, except in the 4th case where 4 x 4 FRF matrix is used for force reconstruction and the last response is used for validation. The standard deviation which results in the minimum sum of errors at each frequency is used in the reconstruction of forces in this 4th case.

3.7 Force reconstruction

The variation of bias error and variance with respect to the number of iterations for one of the frequencies is shown in Figure 13. The iteration number where these two errors coincide is taken as cut-off iteration number. Figure 14 shows cut-off iteration numbers for each of the frequencies. The reconstructed force 1 is shown in Figures 15a-d for all the four cases. The strategy based on a common standard deviation results in an underestimation at many frequencies and an overestimation near the first resonance (Figure 15a). The use of individual standard deviations does not make much difference in the force reconstruction (compare Figure 15a and 15b). When 25% of the response is used as the standard deviation, the reconstruction is much superior and is comparable to Tikhonov regularization result (compare Figure 15c and Figure 1d). Using the percentage of the response found from the validation as the standard deviation results in a similar reconstruction as when 25% of the response is used (compare Figure 15d and Figure 15c). However, there is a spiky reconstruction near the first resonance which is due to the fact that many possible force reconstructions would also lead to good response predictions in this region (first resonance).

The reconstructed forces 2-4 show same trends as seen from Figures 16-18. The force reconstruction is also shown in 1/3 octave band representation in Figures 19a-d. Again, as can be seen the fixed percent of response used as standard deviation gives superior results (Figures 16c-d). The optimum percentage of the response used as standard deviation in the simulation of the 4th case is shown in Figure 20. It can be seen to vary between 10% and 50%.

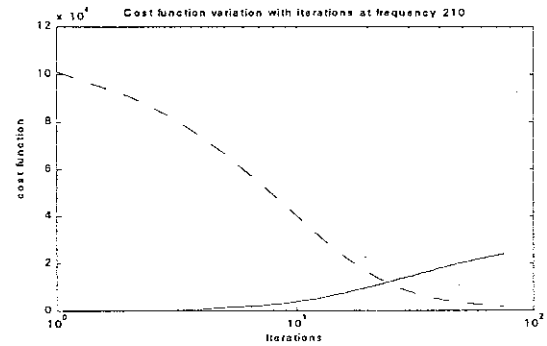

Figure 13. The bias error and variance as function of iterations. _____ bias, _ _ _ _ variance.

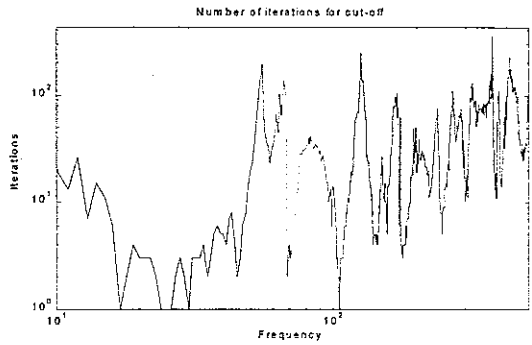

Figure 14. Number iterations for cut-off where bias error and varaince coincide

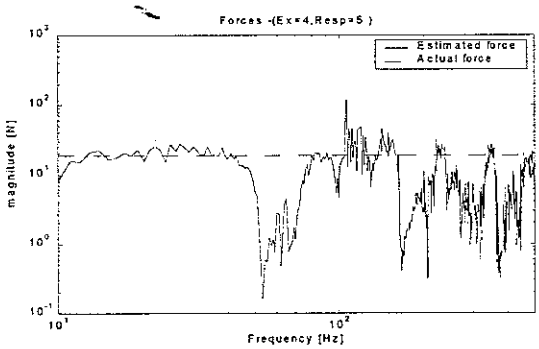

Figure 15a. Force 1 Iterative inversion with common standard deviation for all responses

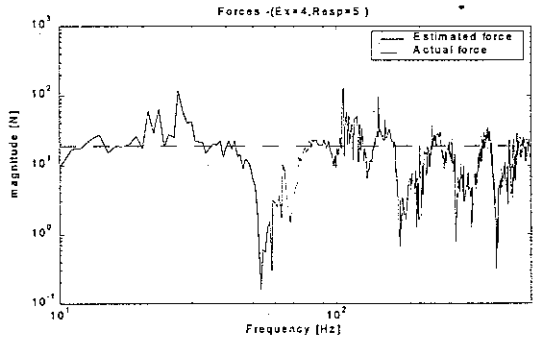

Figure 15b. Force 1 Iterative inversion with standard deviation in each of the responses

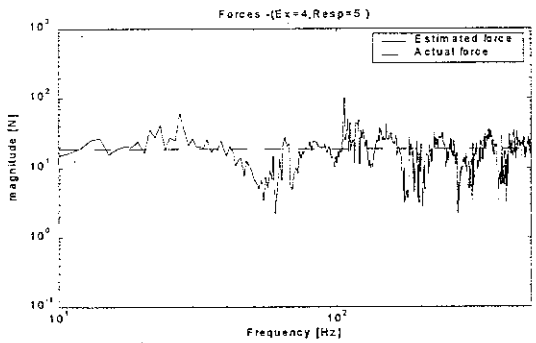

Figure 15c. Force -1 Iterative inversion with standard deviation taken as fixed percentage (25%) of responses

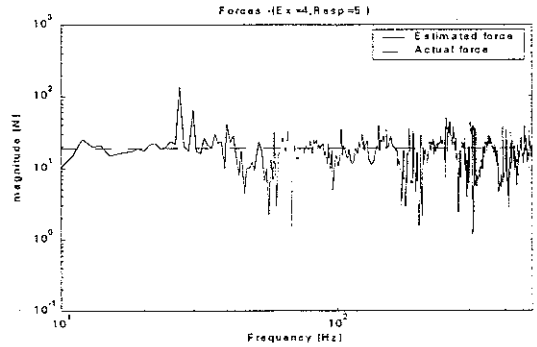

Figure 15d. Force -1 Iterative inversion with standard deviation taken as fixed percentage (up to 50% and validated) of responses.

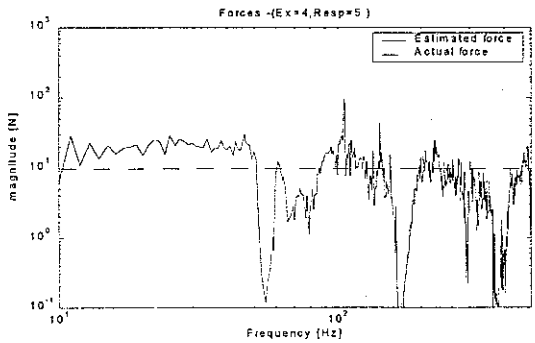

Figure 16a. Force 2 Iterative inversion with common standard deviation for all responses

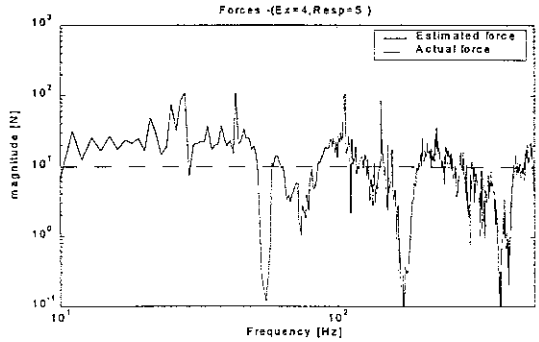

Figure 16b. Force 2 Iterative inversion with standard deviation in each of the responses

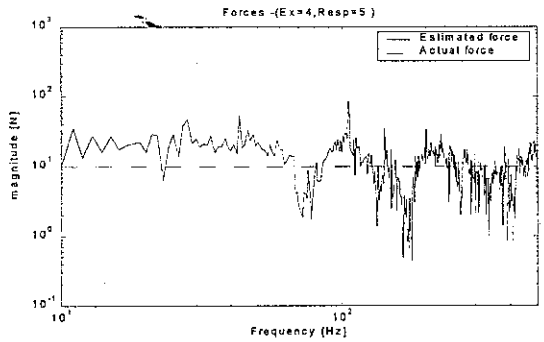

Figure 16c. Force 2 Iterative inversion with standard deviation taken as fixed percentage (25%) of responses

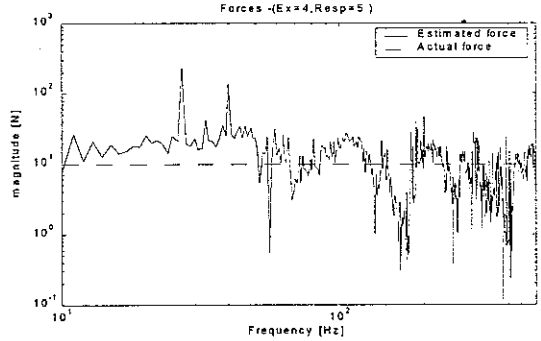

Figure 16d. Force 2 Iterative inversion with standard deviation taken as fixed percentage (up to 50% and validated) of responses

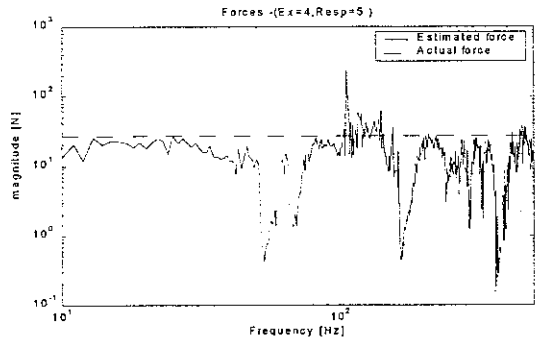

Figure 17a. Force 3 Iterative inversion with common standard deviation for all responses.

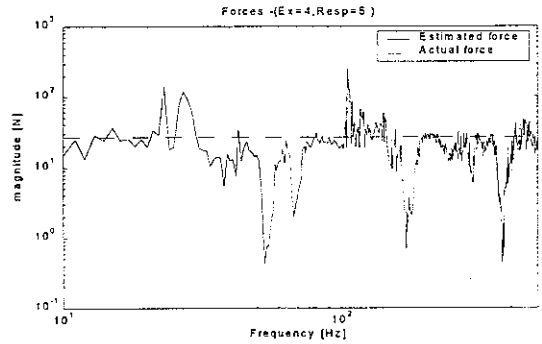

Figure 17b. Force 3 Iterative inversion with standard deviation in each of the responses

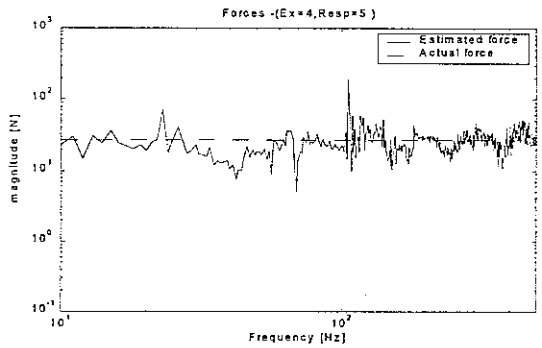

Figure 17c. Force 3 Iterative inversion with standard deviation taken as fixed percentage (25%) of responses

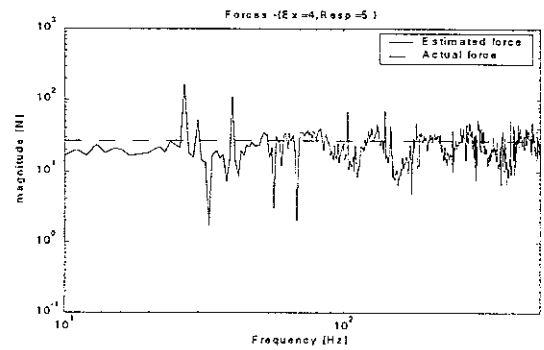

Figure 17d. Force 3 Iterative inversion with standard deviation taken as fixed percentage (up to 50% and validated) of responses

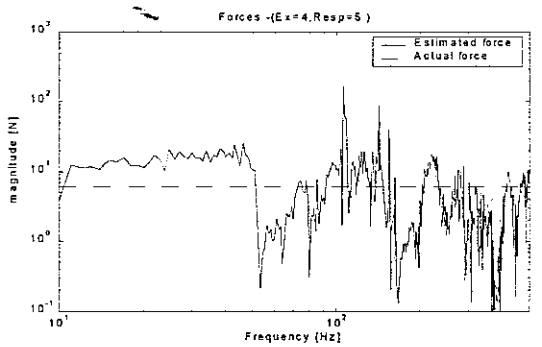

Figure 18a. Force 4 Iterative inversion with common standard deviation for all responses

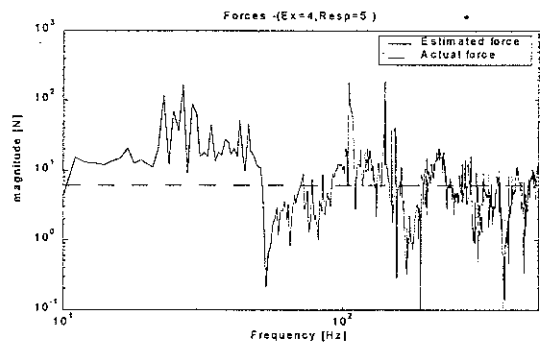

Figure 18b. Force 4 Iterative inversion with standard deviation in each of the responses

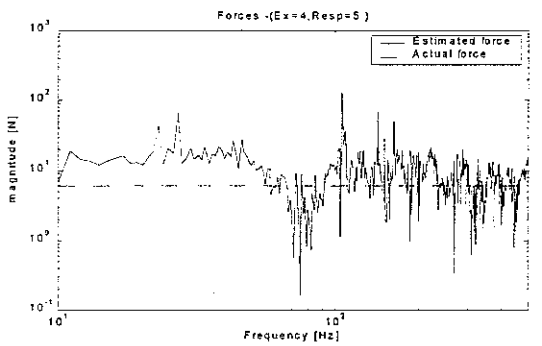

Figure 18c. Force 4 Iterative inversion with standard deviation taken as fixed percentage (25%) of responses

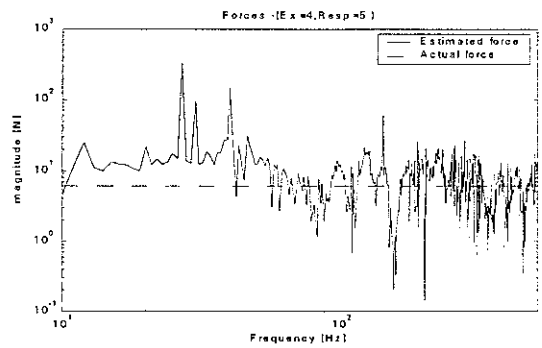

Figure 18d. Force 4 Iterative inversion with standard deviation taken as fixed percentage (up to 50% and validated) of responses

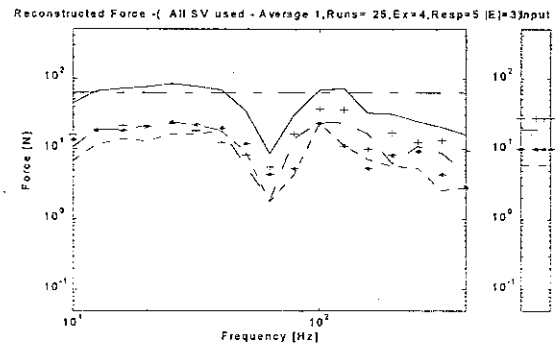

Figure 19a. 1/3 octave band reconstructed forces for iterative inversion with common standard deviation for all responses

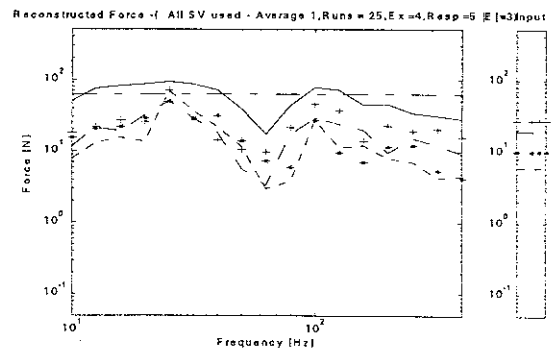

Figure 19b. 1/3 octave band reconstructed forces for iterative inversion with standard deviation in each of the responses

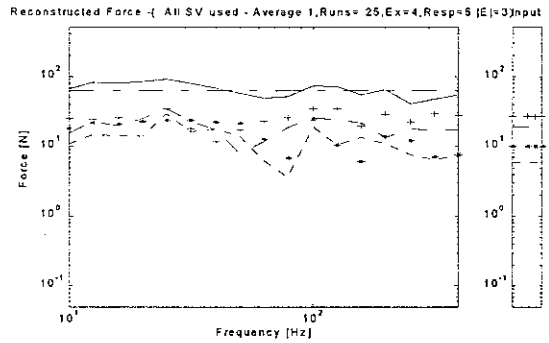

Figure 19c. 1/3 octave band reconstructed forces for iterative inversion with standard deviation taken as fixed percentage (25%) of responses

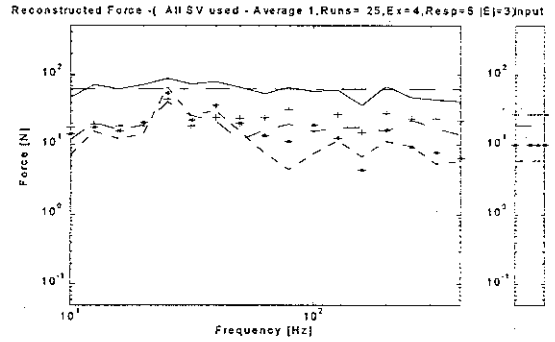

Figure 19d. 1/3 octave band reconstructed forces for iterative inversion with standard deviation taken as fixed percentage (up to 50% and validated) of responses

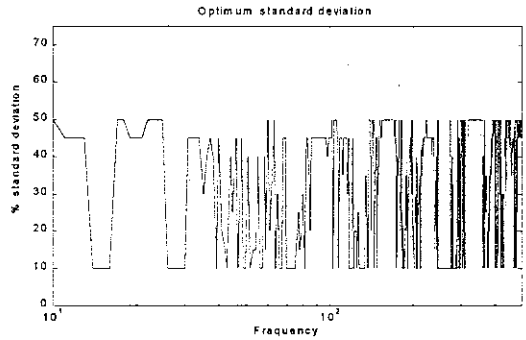

Figure 20. Standard deviations which result in minimum validation error

3.8 Velocity at the receiver location

Figures 21a-d show the 1/3 octave band velocity response contribution at the receiver location from force 1. The velocity contribution calculated with the variable percentage of response used as the standard deviation determined using validation results in the least error compared to all other strategies (compare 21d with 21a-c). The prediction is slightly superior to that of Tikhonov regularization (compare Figure 21d and Figure 6d).

The similar trend is observed in contribution of forces 2-4 to the velocity response. The contributions from forces 2-4 are shown in Figures 22-24.

The velocity response due to all forces at the receiver location for all four cases are shown in 25a-d. The prediction with the variable percentage of response used as the standard deviation determined using validation follows the actual response more closely than others (compare 25d with 25a-c). This prediction is superior to that of Tikhonov regularization in the higher frequency range (compare Figure 25d and Figure 10d). This is also evident when represented in 1/3 octave bands (compare Figure 26d and 11d).

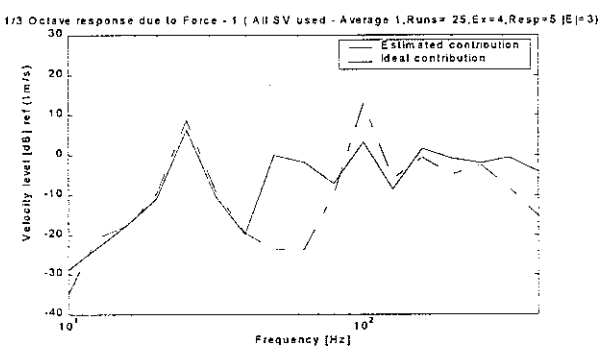

Figure 21a. 1/3 octave velocity response contribution from Force 1 Iterative inversion with common standard deviation for all response

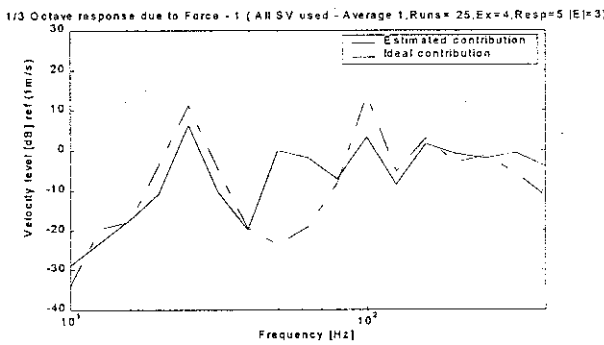

Figure 21b. 1/3 octave velocity response contribution from Force 1 Iterative inversion with standard deviation of each response

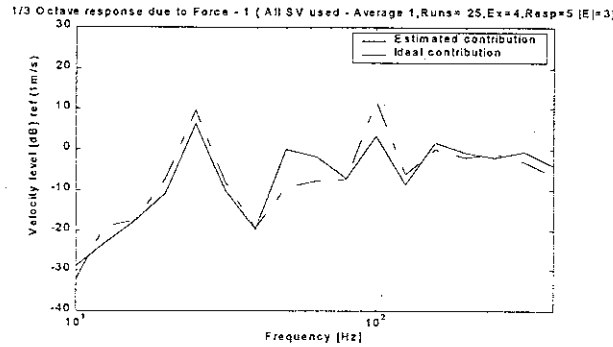

Figure 21c. 1/3 octave velocity response contribution from Force 1 Iterative inversion with standard deviation taken as fixed percentage (25%) of responses

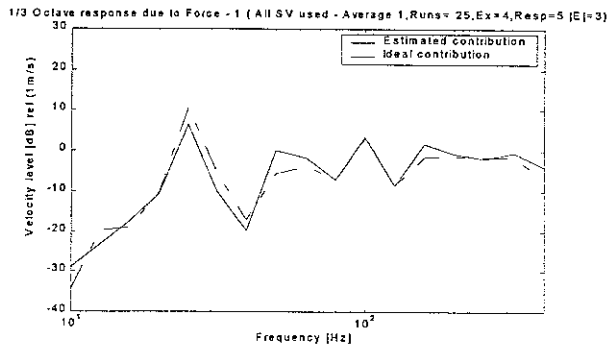

Figure 21d. 1/3 octave velocity response contribution from Force 1 Iterative inversion with standard deviation taken as fixed percentage (up to 50% and validated) of responses

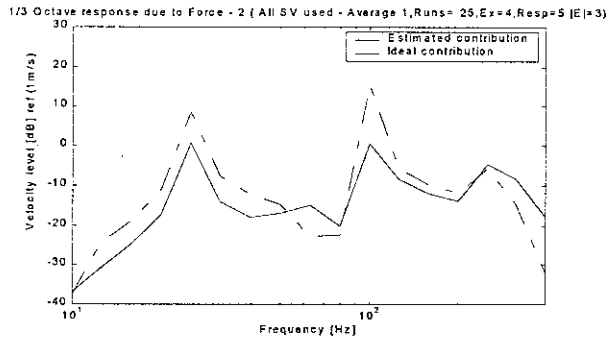

Figure 22a. 1/3 octave velocity response contribution from Force 2 Iterative inversion with common standard deviation for all response

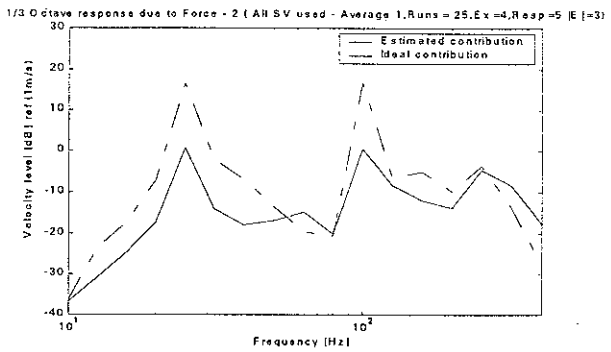

Figure 22b. 1/3 octave velocity response contribution from Force 2 Iterative inversion with standard for each response

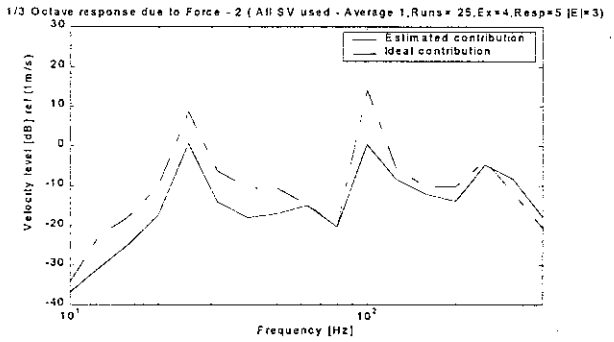

Figure 22c. 1/3 octave velocity response contribution from Force 2 Iterative inversion with standard deviation taken as fixed percentage (25%) of responses

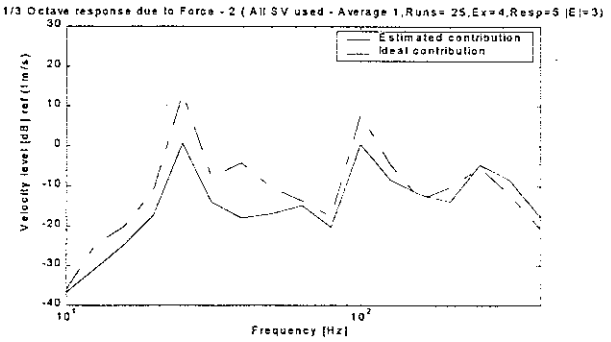

Figure 22d. 1/3 octave velocity response contribution from Force 2 Iterative inversion with standard deviation taken as fixed percentage (up to 50% and validated) of responses

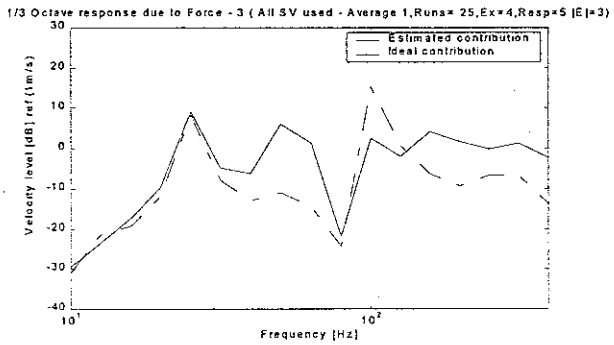

Figure 23a. 1/3 octave velocity response contribution from Force 3 Iterative inversion with common standard deviation for all response

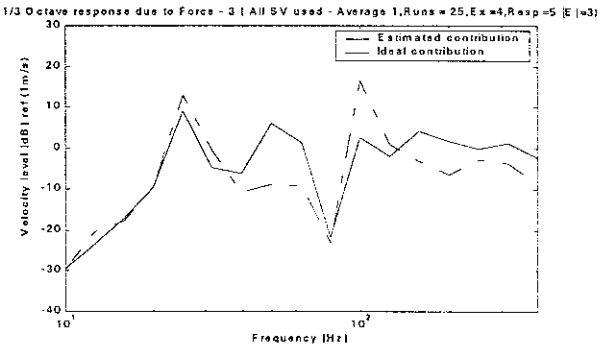

Figure 23b. 1/3 octave velocity response contribution from Force 3 Iterative inversion with standard deviation for each response

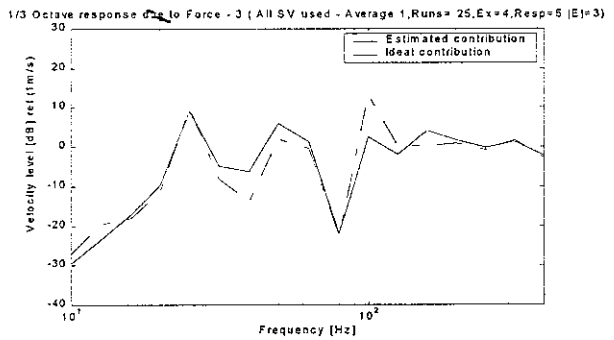

Figure 23c. 1/3 octave velocity response contribution from Force 3 Iterative inversion with standard deviation taken as fixed percentage (25%) of responses

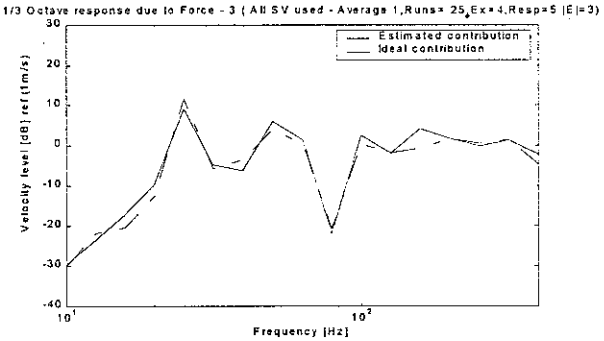

Figure 23d. 1/3 octave velocity response contribution from Force 3 Iterative inversion with standard deviation taken as fixed percentage (up to 50% and validated) of responses

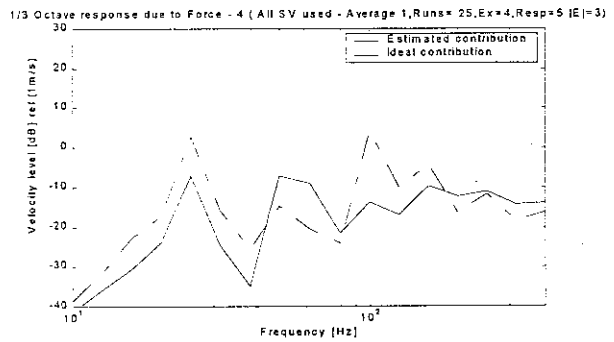

Figure 24a. 1/3 octave velocity response contribution from Force 4 Iterative inversion with common standard deviation for all response

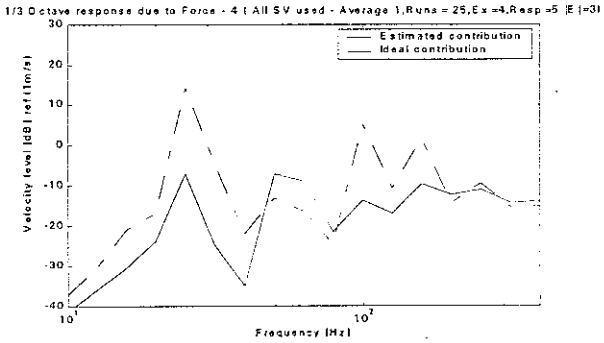

Figure 24b. 1/3 octave velocity response contribution from Force 4 Iterative inversion with standard deviation for each response

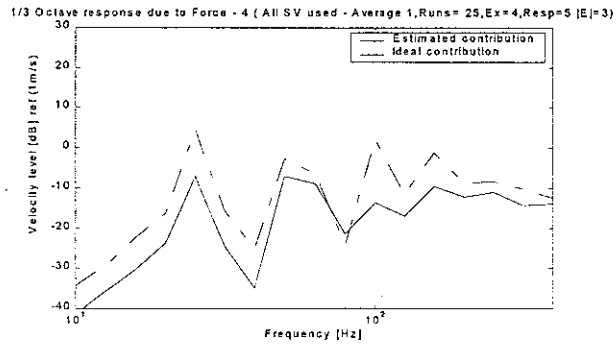

Figure 24c. 1/3 octave velocity response contribution from Force 4 Iterative inversion with standard deviation taken as fixed percentage (25%) of responses

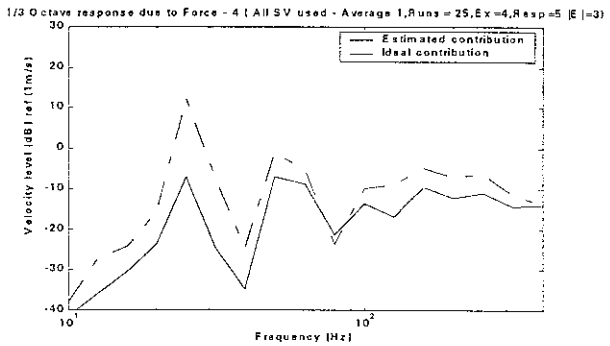

Figure 24d. 1/3 octave velocity response contribution from Force 4 Iterative inversion with standard deviation taken as fixed percentage (up to 50% and validated) of responses

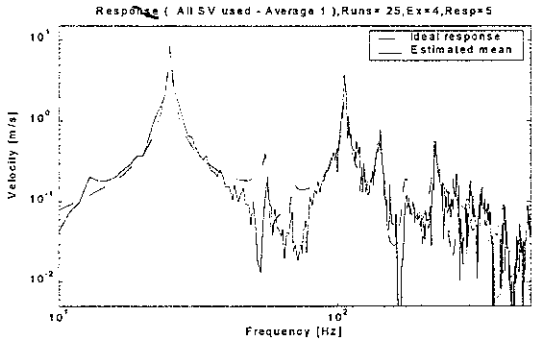

Figure 25a. Velocity response at the receiver location - Iterative inversion with common standard deviation for all responses

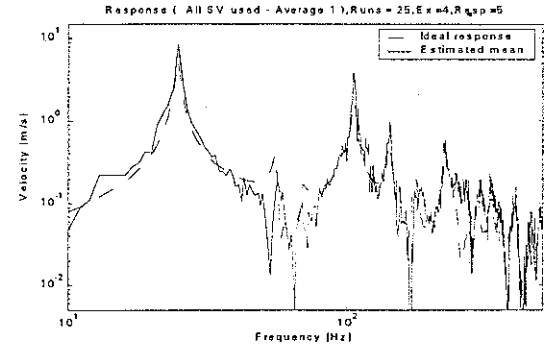

Figure 25b. Velocity response at the receiver location - Iterative inversion with standard deviation for each response

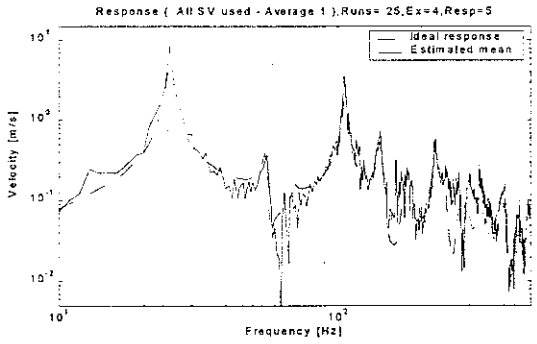

Figure 25c. Velocity response at the receiver location - Iterative inversion with standard deviation taken as fixed percentage (25%) of responses

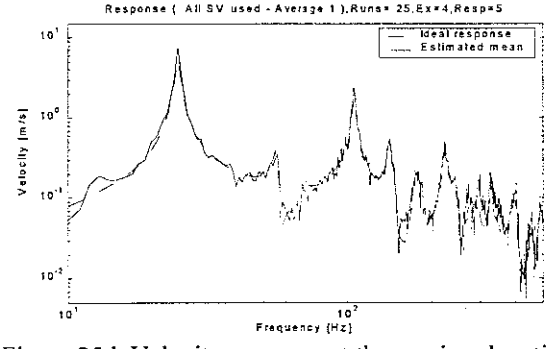

Figure 25d. Velocity response at the receiver location - Iterative inversion with standard deviation taken as fixed percentage (upto 50% and validated) of responses

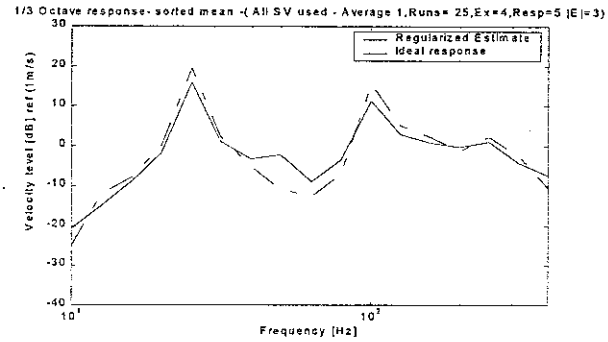

Figure 26a. 1/3 octave band velocity response at the receiver location - Iterative inversion with common standard deviation for all responses

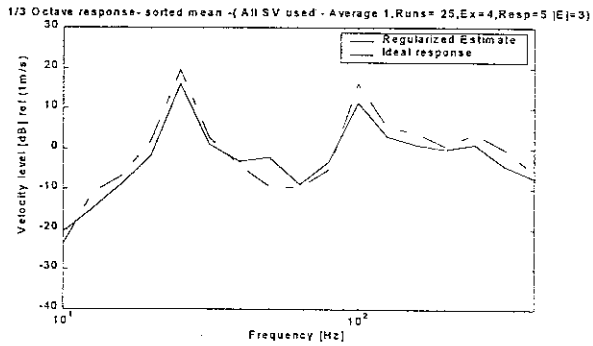

Figure 26b. 1/3 octave band velocity response at the receiver location - Iterative inversion with standard deviation for each response

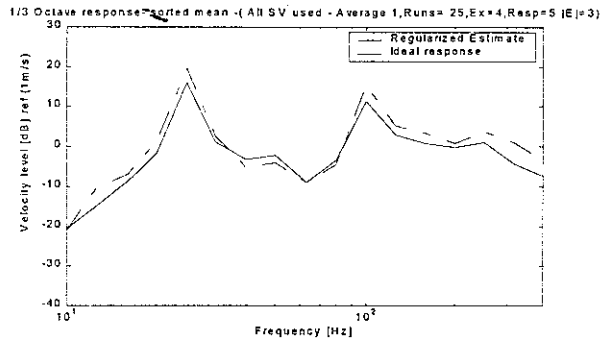

Figure 26c. 1/3 octave band velocity response at the receiver location - Iterative inversion with standard deviation taken as fixed percentage (25%) of responses

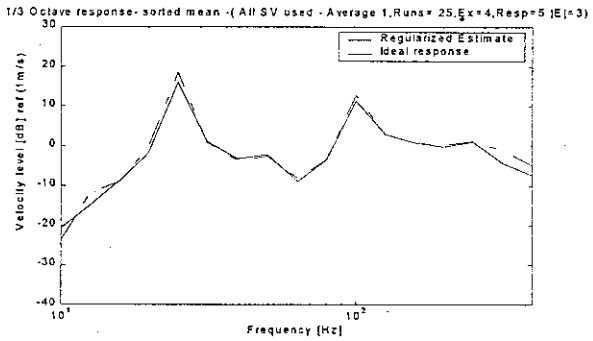

Figure 26d. 1/3 octave band velocity response at the receiver location - Iterative inversion with standard deviation taken as fixed percentage (up to 50% and validated) of responses

3.9 Summary

Using an example of a 5 x 4 FRF matrix it has been shown that iterative inversion based on assumption of a fixed percentage of the response as the standard deviation alongwith validation gives superior results to other iterative inversion schemes.

To quantify the above comparison, the table 2 given below shows the average 1/3 octave band error (in dB) in the velocity prediction by each of the methods.

Table 2 - Summary of results (Average 1/3 octave band errors in dB)

Method	Force 1 (19N) contribution	Force 2 (10N) contribution	Force 3 (27N) contribution	Force 4 (6N) contribution	Total contribution	Rank
Common std deviation	5.9	5. 6	6.9	6.6	2.8	3
Individual std deviation	5.9	7.0	5.3	8.2	2.8	4
25% of resp as std deviation	3.1	4.9	2.7	6.4	2.4	2
10 to 50% of resp as std deviation	2.3	4.9	1.7	6.7	1.2	1

4. Conclusions

Using numerical simulations, force reconstruction and transfer path analysis has been carried in continuation of the earlier work [5-6]. In this study regularization techniques are investigated for force reconstruction and the contributions of individual forces to the response at the receiver location are compared. The Tikhonov regularization is implemented based on an ordinary cross validation scheme for choosing the regularization parameter. In the second study, iterative inversion is investigated for force reconstruction. Bias error and variance are used to arrive at an optimum number of iterations. The following conclusions are drawn based on these simulations,

1. Tikhonov regularization results in better reconstruction of individual forces and their contribution compared to the singular value rejection or resampling of the accelerance matrix.

2. The iterative inversion based on a common standard deviation under-estimates the forces near antiresonances. The solution is biased to a large extent. In fact singular value rejection based contributions are less over-estimated than this case.

3. Even when the individual measured response standard deviations are used, the force reconstruction is similar.

4. By assuming a fixed percentage of the responses as the standard deviation a flexible scheme is developed by which force reconstruction can be controlled. The results with the concept of validation error are better compared to Tikhonov regularization based on ordinary cross validation.

5. References

1. M.H.A. Janssens, J.W. Verheij and D.J. Thompson 1999 Journal of sound and vibration 226, 305-328. The use of an equivalent forces method for the experimental quantification of structural sound transmission.

2. LMS application notes on transfer path analysis 1995. The qualification and quantification of vibro-acoustic transfer paths.

3. JW Verheij, Inverse and reciprocity methods for machinery noise source charectrization and sound path quantification, Part 1 : Sources. International Journal of Acoustics and Vibration, Vol 2, No1, 11-20 1997.

4. JW Verheij, Inverse and reciprocity methods for machinery noise source charectrization and sound path quantification, Part 2 : Transmission paths. International Journal of Acoustics and Vibration, Vol 2, No3, 103-112 1997.

5. AN Thite and DJ Thompson, Study of indirect force determination and transfer path analysis using numerical simulations for a flat plate. ISVR Technical memorandom no. 851, May 2000.

6. AN Thite and DJ Thompson, Further study of indirect force determination and transfer path analysis using numerical simulations for a flat plate. 2nd report.

7. MHA Janssens, JW Verheij and T Loyau, Experimental example of the pseudo-forces method used in characterisation of a structure-borne sound source. Paper submitted to Applied acoustics.

8. JA Fabunmi and FA Tasker, Advanced Techniques for measuring structural mobilities. ASME Journal of Vibration, Acoustics, Stress and Reliability in Design, 345-349, Vol. 110, July 1988.

9. J Biemond, RL Lagendijk and RM Mersereau, Iterative Methods for Image processing. Proceedings of the IEEE, Vol. 78, No. 5, May 1990.

10. PA Nelson, Some inverse problems in acoustics. Sixth international congress on sound and vibration, 5-8 July 1999, 7-32.

11. PA Nelson and SH Yoon, Estimation of acoustic source strength by inverse methods: Part I, conditioning of the inverse problem. Journal of sound and vibration (2000) 233(4), 643-668.

12. SH Yoon and PA Nelson, Estimation of acoustic source strength by inverse methods: Part II, Experimental investigation of methods for choosing regularization parameters.Journal of sound and vibration (2000) 233(4), 669-705.

13. PA Nelson and SJ Elliott, Active Control of Sound, 416-420 : Academic press, London, 1992.

14. DM Allen, The relationship between variable selection and data augmentation and a method for prediction. Technometrics 16, 125-127, 1974.

15. BK Kim and JG Ih, Design of an optimal wave vector filter for enhancing the resolution of reconstructed source field by near-field acoustical holography (NAH). JASA, 3289-3297, 107 (6), 2000.

16. A Tikhonov and V Arsenin, Solution of Ill-Posed Problems : Winston, Washington DC, 1977.

17. NP Galatsanos and AK Katsaggelos, Methods for choosing the regularization parameter and estimating the noise variance in image restoration and their relation. IEEE transactions on Image procesing, 322-336, Vol. 1, No. 3, July 1992.